IEEE Access
Multidisciplinary ⋮ Rapid Review ⋮ Open Access Journal

Received 13 September 2023, accepted 12 November 2023, date of publication 20 November 2023,
date of current version 29 November 2023.

Digital Object Identifier 10.1109/ACCESS.2023.3334620

TOPICAL REVIEW

Prediction of Electric Vehicle Driving Range and Performance Characteristics: A Review on Analytical Modeling Strategies With Its Influential Factors and Improvisation Techniques

AZHAGANATHAN GURUSAMY[1], BRAGADESHWARAN ASHOK[1], AND BYRON MASON[2]
[1]School of Mechanical Engineering, Vellore Institute of Technology, Vellore, Tamil Nadu 632014, India
[2]Department of Aeronautical and Automotive Engineering, Loughborough University, LE11 3TU Loughborough, U.K.

Corresponding authors: Bragadeshwaran Ashok (ashokmts@gmail.com) and Byron Mason (B.Mason2@lboro.ac.uk)

This work was supported in part by the Royal Academy of Engineering under Grant ESMN 2123/2/93 and Grant DIA-2022-150, and in part by Engineering and Physical Sciences Research Council (EPSRC) Project under Grant EP/L014998/1.

ABSTRACT Electric mobility is getting prominence in modern transportation as government policies aim to reduce greenhouse gas (GHG) emissions. In the context of real-time testing, numerical modelling and simulation of electric vehicle (EV) powertrains play a vital role in developing an efficient electric powertrain and charging infrastructure as it consumes less time and cost. Also, it enhances the overall performance by optimizing the size and configuration of the EV powertrain under different driving conditions. Thus, the review paper explores the different modelling approaches used for estimating the energy consumption (EC) and driving range (DR) initially. Further, the vehicle analytical model is discussed in detail with sub-models of powertrain components and vehicle dynamics, which have the mathematical correlation related to power losses and energy flow. Additionally, the necessity, development process, characterization and accuracy of localized driving cycles (DCs) and commonly used driver controller models for EVs are critically elaborated. Further, the impact of various influential input parameters such as vehicle parameters and driving conditions on EV performance characteristics is analyzed along with different improvisation methods utilized in the existing literature. From this extensive review, it can be concluded that simulation results by using an analytical vehicle model have good accuracy with chassis dynamometer-based testing and it can be used for optimizing the size and configuration of EV powertrain components under different scenarios. Finally, the present status and future research required in the field of EV powertrain development through modelling and simulation are summarized to extend the application of EVs in transportation sectors.

INDEX TERMS Electric vehicle, modelling and simulation, analytical vehicle model, driving range, energy consumption.

ABBREVIATION AND NOMENCLATURE

A_{ave}, Average acceleration; BLDC motor, Brushless direct-current motor; CVT, Continuously variable transmission; D_{ave}, Average deceleration; DC, Driving cycle; D_{cyc}, Drive cycle distance; DMMCP, Dual-motor with multi-mode coupling powertrain; DOD, Depth-of-discharge; DR, Driving range; E2W, Electric-2-wheelers; E3W, Electric-3-wheelers; E4W, Electric-4-wheelers; EC, Energy consumption; ECP, Equivalent circuit parameters; EM, Electric motor; EMS, Energy management system; EPA, Environmental protection agency; ERDC, E-rickshaw driving cycle; EV Electric vehicle; EVIDC, New driving cycle for e-rickshaws; FEM, Finite element method; FTP, Federal test procedure; GHG, Greenhouse gas; G2V, Grid-to-vehicle; HWEFT, Highway fuel economy test cycle; IDC, Indian driving cycle; IM, Induction motor; N.V, Nominal voltage; NEDC, New european driving cycle; NVH, Noise, vibration and harshness; P_A, Percentage

The associate editor coordinating the review of this manuscript and approving it for publication was Chaitanya U. Kshirsagar.

of acceleration duration; PAM, Pulse amplitude modulation; P_C, Percentage of cruising duration; P_D, Percentage of deacceleration duration; P_I, Percentage of idling duration; PID, Proportional–integral–derivative; PMSM, Permanent magnet synchronous motor; PVM, Power-based vehicle model; PWM, Pulse width modulation; RMS, Root mean square; SE2WC, Shanghai electric two-wheeler cycle; Si IGBT, Silicon-based power converters and insulated-gate bipolar transistor; SiC MOSFET, Silicon carbide metal–oxide–semiconductor field-effect transistor; SOC, State-of-charge; SRM, Synchronous reluctance motor; STR, Source-to-range; T.R, Transmission ratio; T_{cyc}, Drive cycle time duration; UDDS, Urban dynamometer driving schedule; V_{ave}, Average velocity; V_{max}, Maximum velocity; VRP, Vehicle routing problem; UC, Ultra-capacitor; WLTC, Worldwide harmonized light vehicles test cycle.

I. INTRODUCTION

According to the global EV outlook 2022, electric mobility can be a primary driving force to ensure the decarbonised transportation sector, which contributes a high share of GHG emissions globally. Especially, road vehicles driven by fossil fuels contribute about 74.5% of greenhouse emissions among other transportation sectors. Also, global EV sales in 2022 have increased by about 13%, which indicates the direction of road mobility is put a path to achieve net zero emission by 2050 and sustainable development goals [1]. As of now, battery and fuel cell EVs are considered as final step of the electric revolution in the transportation sector, whereas it has evolved with the different variants of hybrid electric vehicles [2], [3]. The salient features of EV powertrains over conventional powertrains are higher well-to-wheel efficiency, urban accessibility, comfort and reliability with zero tailpipe emissions and less maintenance due to simple and efficient powertrain design [4], [5]. Therefore, the autonomy of EVs should be cautiously designed as they play a vital role in public transport of smart cities as shared mobility [6], [7]. Moreover, EVs are classified by their powertrain autonomy such as electric powertrain with and without transmission along with the position of the motor like conventional, in-wheel and hub-mounted [8], [9]. The outline of EV powertrain architecture with the key components such as power source (battery), power electronics, motor, transmission, final drive and different controllers are presented in Fig. 1. The selection of electric powertrain size and configuration should satisfy the vehicle performance requirements with considering vehicle constraints and power source variables. Currently, the simple electric drivetrain with a Li-ion battery as a power source is used for vehicle applications [12], [13], [14]. Also, electric motors (EM) like brushless direct-current (BLDC), induction (IM), synchronous reluctance (SRM), and permanent magnet synchronous (PMSM) motors are chosen according to the vehicle performance requirement, space availability, noise, vibration and harshness (NVH) characteristics. Also, the power electronics and different control systems in EVs are to ensure the maximum performance of the traction motor, battery and charger [15], [16], [17]. Recently, a lot of research has been initiated into developing high energy density and fast charging capability batteries with lightweight materials and smart charging modes to eliminate the range anxiety of drivers. Also, the development of advanced technologies related to bi-directional power flow such as grid-to-vehicle (G2V), vehicle-to-grid and vehicle-to-everything communications has provided more flexibility during the charging and discharging process [18], [19]. Recently, electric powertrains with high energy density motors and multi-speed transmission systems have gained attraction to enhance overall performance [20], [21].

The continuous technical improvements of electric powertrain demand to assess the EC and DR along with other performance characteristics of EVs. Currently, the development of modelling strategies with different vehicle configurations and simulation scenarios is achievable due to the continuous improvements in computing power capability over recent decades [22]. Moreover, different modelling approaches are focused on considering the influence of the size and configuration of the electric powertrain, energy management system (EMS) and atmospheric conditions on EV performances with a specified scientific tool as per the analysis requirement [23], [24]. The modelling process of the EV powertrain involves data collection, developing the mathematical correlation related to each powertrain component and making proper signal flow between each sub-model [25]. In overall, the modelling process can be categorised into analytical and data-driven according to the computation methodologies used [26]. The functionality, advantages and disadvantages of these models are shown in Fig. 2. Further, the analytical vehicle model is classified into power-based vehicle model (PVM), vehicle routing problem (VRP) and source-to-range (STR). Whereas the PVM is assessing the EV performances based on the power balance between the electric powertrain through microsimulation and it is further extended to study the charging performances and variation in EC due to traffic flow with GPS data [22], [27]. In VRP modelling, the EC and DR are assessed for selected routes with constant and average values of vehicle acceleration and deceleration. The effect of powertrain dynamics and EMS algorithm are neglected in this approach to avoid complexity in computation [28]. The STR modelling approach is used to evaluate the environmental effects through life cycle analysis by considering all the manufacturing processes of powertrain components [29]. It can be used to optimize the EV powertrain to identify the most energy-demanding process and suggest alternative new processes at a specific region [30].

Data-driven analysis is another primary approach to evaluate EV performances, which is more suitable for analyzing the large quantity of real-time data in absence of a vehicle model [37], [38]. This approach is to study the interaction effect of different vehicle input variables by considering the influence of different traffic congestion and driving behaviours [39], [40]. However, the accuracy of

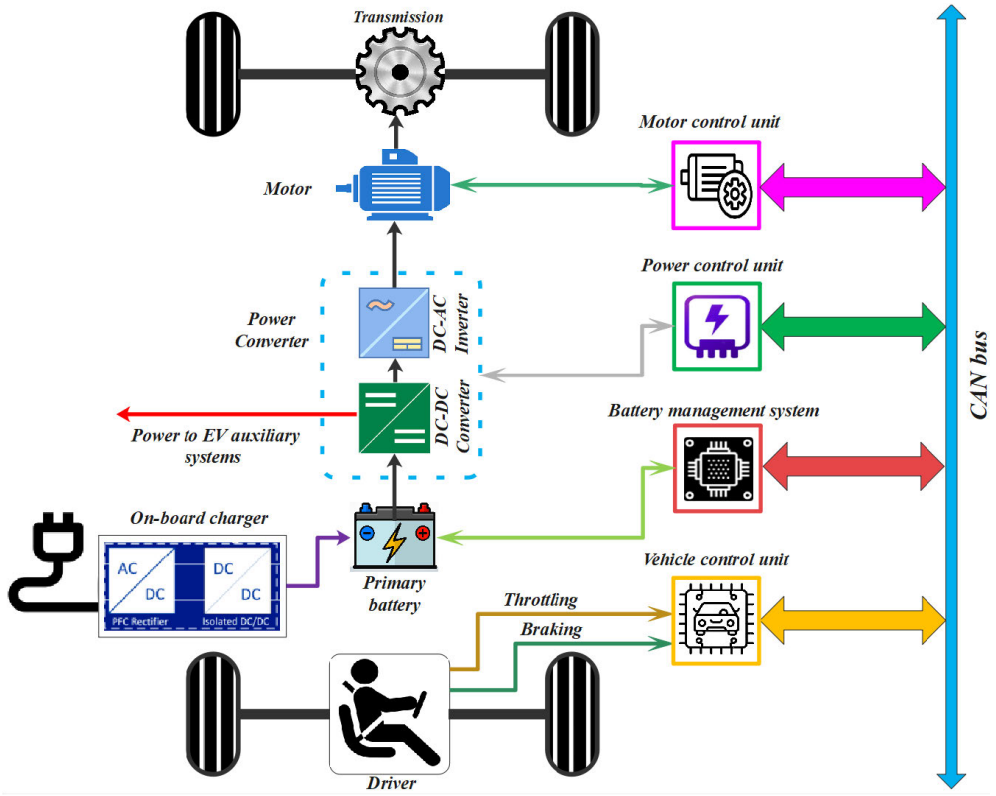

FIGURE 1. Structural outline of EV powertrain with different control units [10], [11].

EV performance evaluation through data-driven analysis is predominately reliable on the quality of the data processing phase. Besides, it can be ensured by various modern computing techniques like genetic algorithms, artificial neural networks and machine learning [41], [42], [43]. By comparing the modelling approaches, it is evident that analytical model-driven approaches are more appropriate to evaluate the EV performance entities by considering the different technical details of EVs with less error and computation effort [44]. The modelling and simulation process with the appropriate modelling strategy requires suitable simulation software. Further, it can be chosen based on the typical EV performance evaluation such as vehicle system and control analysis, G2V with renewable energy, EMS, charge scheduling and traffic systems [45], [46]. The simulation tools play a vital role in evaluating the EV performance in different scenarios by reducing time consumption, cost and human effort associated with real-time testing. However, the accuracy of simulation results is unfailing on the data quality of powertrain components and vehicle dynamics mathematical model [47], [48]. The primary outputs of EV powertrain simulation are EC and DR. Other than this, the size, operating region and dynamic behaviours of powertrain components can be evaluated for selected DCs to know the limit of powertrain components. In most cases, the error margin of EV performance values through simulation with real-time data is negligible [49], [50]. However, the real-time testing of EVs such as dynamo and road tests plays an equal role to ensure overall EV performances that include safety and reliability [51].

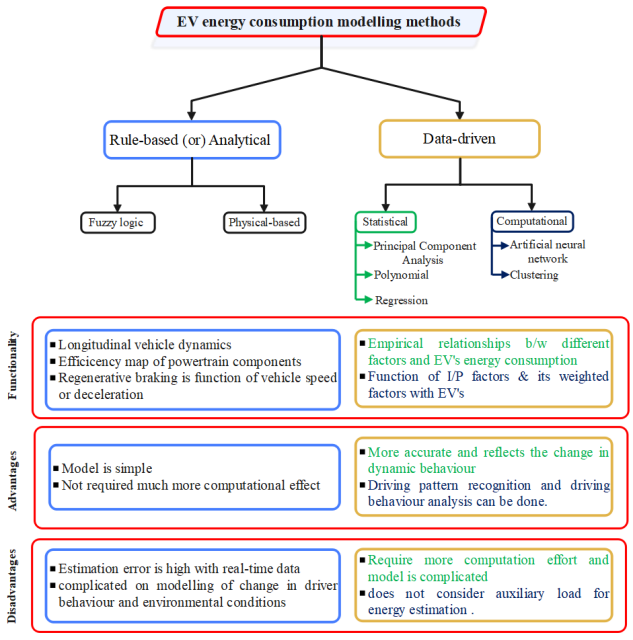

FIGURE 2. Functionality, merits and demerits of different EV driving range modelling approaches [31], [32], [33], [34], [35], [36].

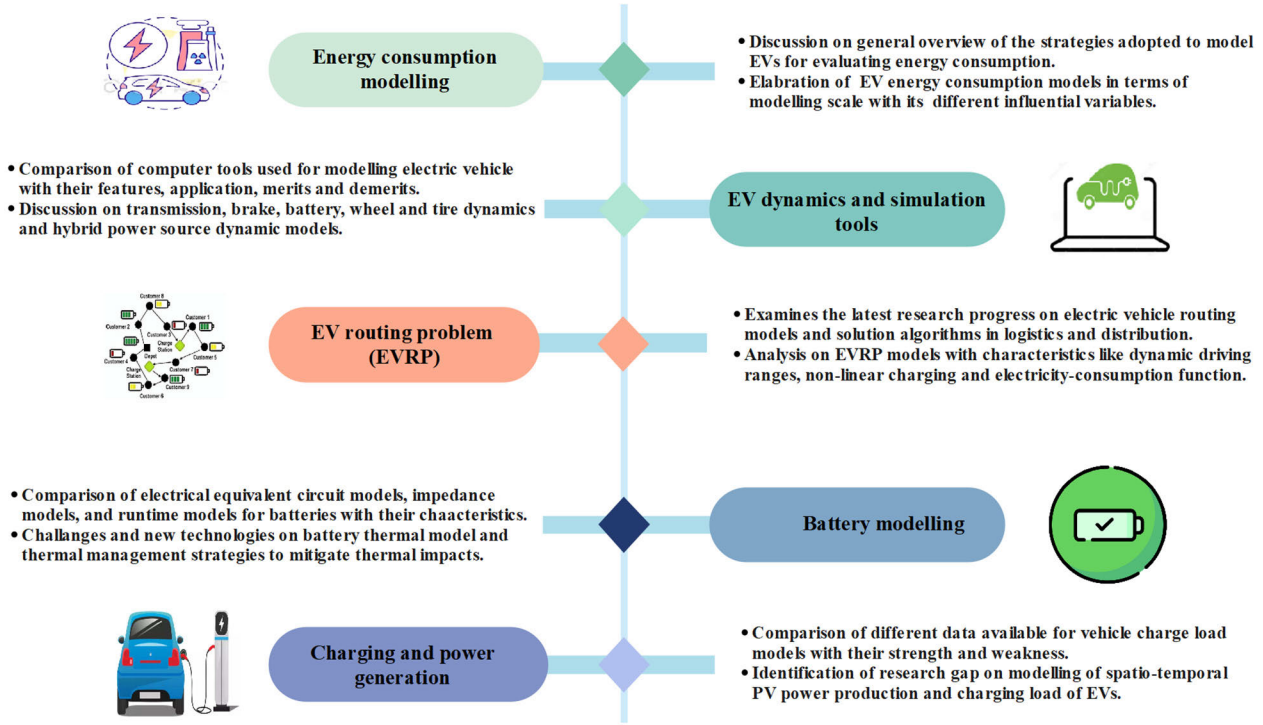

FIGURE 3. Status of existing review work on different modelling strategies of various EV research domains [52], [53], [54], [55], [56], [57], [58], [59], [60].

II. OBJECTIVE AND METHODOLOGY

Over the years, numerous studies have been carried out on numerical simulation of EV performance characteristics at various driving and atmospheric conditions. Particularly, the estimation of accurate DR by evaluating the EC of EVs is the key factor for eradicating driver anxiety and establishing charging infrastructure in region-specific. So, it is more important to understand the different modelling strategies along with simulation tools used for evaluating the EV performance characteristics such as EC, DR, gradeability and acceleration. Since few review articles are published in the open literature to analyze the different modelling strategies and simulation tools used in various research domains of EV as discussed in Fig. 3.

However, there are no studies focused on an in-depth analysis of vehicle analytical modelling approaches for predicting EV energy consumption by considering the different research entities to improve the accuracy of simulation results. Additionally, researchers in the field of EV powertrain development for green mobility should have a clear perspective on different losses by powertrain components at wide operating regions which significantly influences the selection and matching of powertrain components. Also, the standardization of regional DCs needs to understand the characterization of localized driving conditions which improves the reliability of EV performance measurements. Further, the influence of variation in the vehicle, road and ambient parameters on EV performance along with its improvisation methods should be reviewed for optimizing and extending the performance of EV powertrain. To bridge these voids, this review article is framed to provide a critical analysis on the application of the analytical modelling approach for evaluating EV performance through numerical simulation along with the characterization of localized DCs. Fig. 4. illustrates the structural outline of the content discussed in section-wise of this review article. The authors believe that this review may act as a prime platform for the researchers to make use of numerical modelling and simulation for developing efficient EV powertrains.

III. ANALYTICAL VEHICLE MODELLING APPROACHES

Based on the modelling approach and direction of energy flow, the vehicle analytical model is further classified into backward-facing and forward-facing [61]. In the case of the backward-facing model, generalized forces and motions are the inputs and outputs of the powertrain components, which is reversed in the forward-facing modelling approach [62]. The generic structure for backward-facing model consists of sub-models related to DCs, vehicle dynamics and powertrain components. Further, the size of the battery, EC and DR of EVs are estimated in the battery sub-model with the efficiency map and datasheet parameters of powertrain components and vehicle through other sub-models for different DCs [65]. Furthermore, efficiency maps are collected through the testing of real-time powertrain components such as battery, converter, motor and transmission at static conditions. So, backward-facing model is not able to represent the dynamic behaviours of powertrain components.

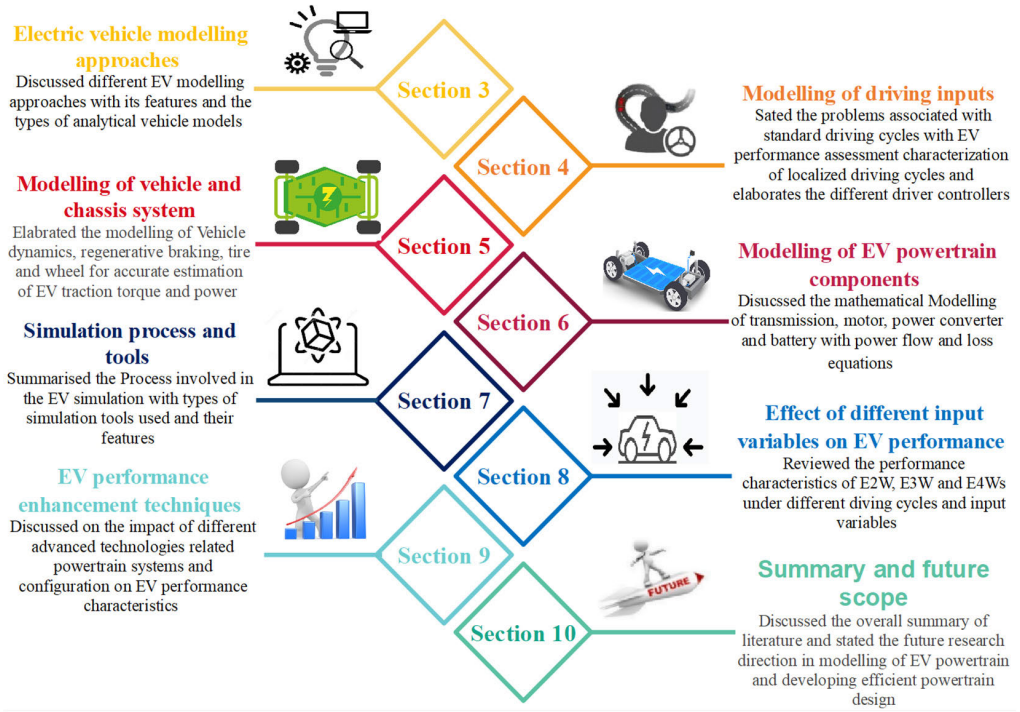

FIGURE 4. Status of existing review work on different modelling strategies of various EV research domains [52], [53], [54], [55], [56], [57], [58], [59], [60].

However, it requires lesser computational effort and time for sizing and optimizing the size of powertrain components by estimating the EC of EVs [26], [66]. Conversely, the forward-facing model is desired to study the dynamic behaviour of the driver and the interaction between powertrain components with their limitations [67]. To accomplish this, the driver sub-model is used as a controller in the forward-facing model as shown in Fig. 5a. to match the vehicle speed with reference speed (DC speed), which is not available in the backward-facing model as shown in Fig. 5b. Further, the error signal from the controller generates the throttle or brake command as a control signal to regulate the torque and speed of the motor. Then, the torque from the traction motor is applied to the wheel through the transmission model [68], [69]. Since the forward-facing model demands more computation effort and time, it can be used for evaluating the EV prototype through hardware in loop testing more easily and rapidly. Additionally, forward-facing model can be used to develop and evaluate the controller and regenerative braking for EVs since it is very realistic in dynamic conditions [70], [71]. Moreover, it is indispensable to understand the different input and output parameters of sub-models used in both approaches for evaluating the EV performances as discussed in the consecutive sections.

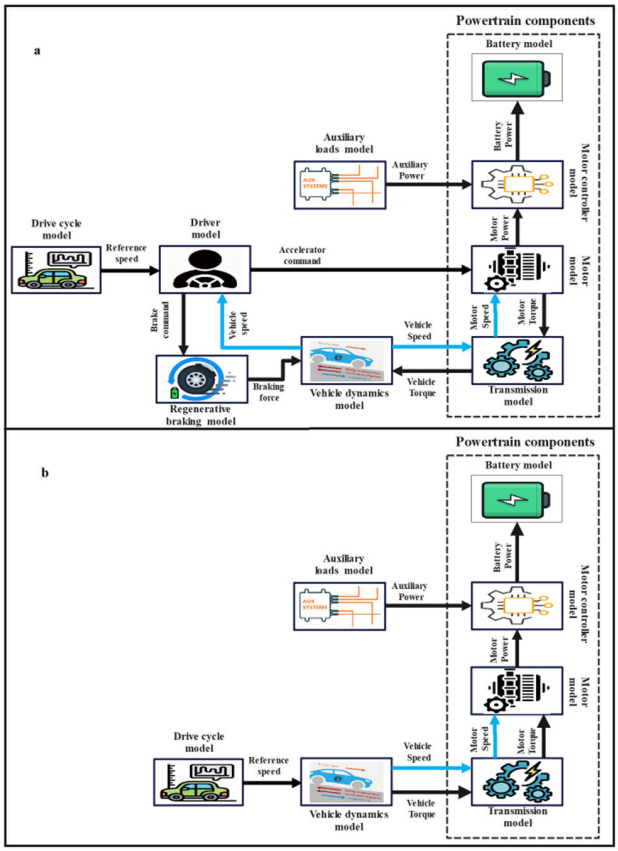

FIGURE 5. Structural overview of forward and backward-facing modelling approaches with sub-models [63], [64].

IV. MODELLING OF DRIVING INPUTS

The primary input of the EV powertrain model for assessing EC and DR is vehicle speed. During modelling, the vehicle speed in the DC sub-model is given in the form of time and

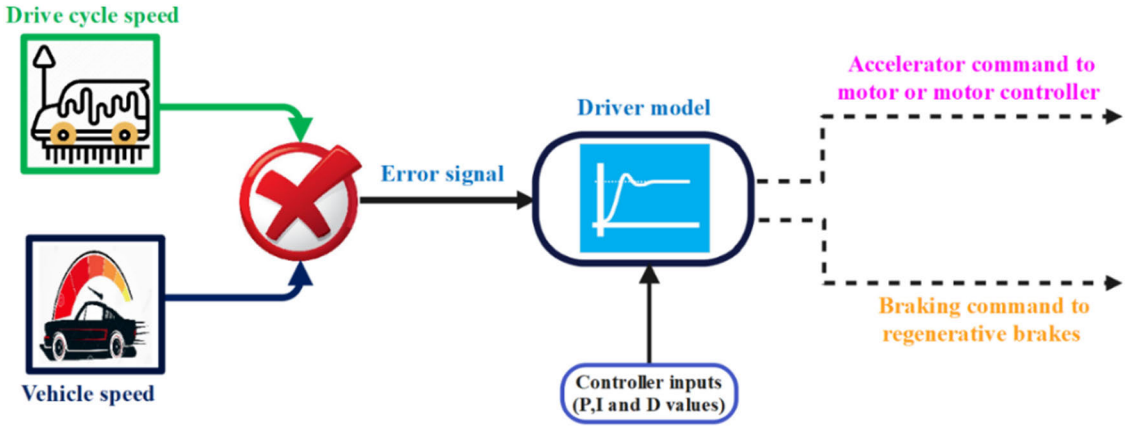

FIGURE 6. Overall functionality of the diver sub-model along with its inputs and outputs.

vehicle velocity profile. Also, the driver unit is modelled in the forward-facing model to match the vehicle speed and DC speed. In this section, the DC model is elaborated with the necessity, development process and characterization of region-specific DCs. Also, the driver model with different control strategies is discussed as follows.

A. DRIVING CYCLE

The EC, DR and sizing of the EV powertrain are assessed by the standard DCs, which are represented as a 2D look-up table consisting of time and vehicle velocity. Commonly, international-legislated DCs based on several driving standards are used in most of the EV performance assessment studies, which are originally developed for fossil-fueled vehicles (FV) [72], [73]. Due to the differences in torque, power and braking characteristics of EVs, the estimated value of EC and DR using standard DCs are not matched with real-time data [74]. To overcome these issues, the localized DCs for EVs in a particular region or city should be developed by the researchers based on the road profile, traffic conditions and vehicle class or type [75], [76]. The development process of DCs for EVs involves route selection, collection and processing of driving data for a particular EV. Further, the selection of drive routes such as urban, rural, sub-urban, and motorway is based on the traffic conditions and vehicle classes [77], [78]. Most commonly, the methods based on random selection, clustering, statistical and Markov chain analysis are used to collect and process the real-time driving data for developing the localized DCs [79]. Further, the accuracy of DC data is ensured by increasing the recording frequency of sample data through the data logging devices [80], [81]. Table 1 elaborates on the characterization of non-legislative or localized DCs for different driving conditions and vehicle classes of EVs and it is evident that the EC of EVs for localized DCs is closely matched with real-time data.

B. DRIVER MODEL

The driver sub-model replicates the driving behaviour of a human realistically. During modelling, deviation in speed (dV) between desired DC speed ($V_{desired}$) and actual vehicle speed ($V_{act.}$) as defined in equation 1. Based on the sign of dV, the driver command for acceleration or deceleration and braking is generated to follow the $V_{desired}$ [90]. In most cases, the driver sub-model has two subsystems such as the driver controller and commands for acceleration and braking. Further, the driver controller signal is given a normalised value between 0 to 1 as input to the accelerator and brake pedal for acceleration and braking [91], [92], [93]. Fig. 6. elaborates on the overall functionality of the diver sub-model along with its inputs and outputs. There are several controllers used for tuning the $V_{act.}$ based on $V_{desired}$ by its response time and ability to minimize the error. In several studies, the PI controller is used in the driver model to regulate the $V_{act.}$ according to the $V_{desired}$ [94], [95]as stated in equation 2.

$$dV = V_{desired} - V_{act.} \tag{1}$$

$$PI\ (S) = \left(I * {}^{1}/_{S}\right) + P \tag{2}$$

Here, S, I and P are the time, integral, proportional gain respectively. However, PID-based controllers are widely used in real-time application as it is very easy to implement with shorter response time and minimum error [96]. Here, the dV is the input for the PID controller and $V_{act.}$ is matched with $V_{desired}$ by tuning the PID controller transfer function such as proportional (K_p), integral (K_i) and derivative co-efficient (K_d) [97] in equation 3.

$$K\ (S) = K_p + \left(\frac{K_i}{S}\right) + (K_d * S) \tag{3}$$

Here, K_p has more influence on the driving behaviour meanwhile the K_i and K_d are used for smoothening of driver behaviour to maintain the $V_{act.}$ closer to Vd_{esired}. Irrespective of the controlling methods and nature of the DCs, the driver controller should maintain the dV in the range of $\pm$ 2 kmph [98], [99].

V. MODELLING OF VEHICLE DYNAMICS

It is essential to understand the total tractive force (F_t), torque (T_t) and power (P_t) required at the wheel for selecting the

TABLE 1. Details on the characterization of localized DCS for different EV configurations.

Vehicle types	Regions	Name of DCs	Methods used	DC characteristics										Comparison in EC (Wh)		Ref.
				T_{cyc} (Sec)	D_{cyc} (Km)	V_{ave} (Km/hr)	V_{max} (Km/hr)	A_{ave} (m/s2)	D_{ave} (m/s2)	Driving phases (time portion of driving modes in %)				Real-world	Developed DC	
										PI	PC	PA	PD.			
E2W	Urban	SE2WC	Markov chains	1704	9.4	21.4	40.4	0.5	-0.45	10.5	33	27.3	29.6	_	_	[82]
	Semi-urban	SE2WC	Up-sampling	1704	9.4	21.4	40.4	0.55	-0.53	9.5	20.2	34.6	35.7	23.4	24.5	[83]
	Rural and semi-urban	EVIDC	micro-trips	1125	4.31	13.79	28.43	0.206	-0.204	21.5	30.6	25.2	22.6	20.87	19.87	[84]
E3W	Rural and urban	ERDC	micro-trips with k-means clustering	980	5.84	17.4	28	1.12	-1.15	15.7	42.5	21.5	20.4	_	_	[79]
		Xi'an	k-means and SVM	1200	38.4	20.74	63.86	0.78	-0.77	17.9	17.3	32.9	31.9	_	_	[85]
		Dublin	Markov chains	1600	_	30.87	84.5	0.62	-0.64	20.7	27.6	26.7	25	_	_	[86]
E4W	Urban	Tianjin	Micro-trips with two-class Fisher's discriminant analysis	1050	_	22.78	_	0.52	-0.55	9	27	34	30	19.23	18.55	[87]
		Xi'an	Markov and Monte Carlo	1200	255	23.82	63.86	0.73	-0.76	10.5	27.4	29.7	32.3	23.1	24.5	[88]
	Urban	Beijing	Kinematics Segments	1150	5.14	23.25	-	-	-	34.5	16.5	25	24	-	-	[78]
	Suburban			1190	11	36.72	-	-	-	9.92	28.3	30.8	31	-	-	
	City	BEV	Markov chains	375	2.5	24	46	-	-	-	-	-	-	11.5	12.2	[89]
	Rural			343	4.4	46	74	-	-	-	-	-	-	13.3	13.3	
	Motrorway			997	18.1	65	103	-	-	-	-	-	-	15.1	14.9	

appropriate size and configuration of the electric powertrain. In this section, the importance and mathematical correlations of vehicle dynamics, wheel and tire sub-models are explained for calculating total tractive requirements to improve the accuracy of EC and DR estimation.

A. VEHICLE PARAMETERS

The vehicle dynamics of EVs are broadly classified into longitudinal, lateral and vertical dynamics, which substantially deal with vehicle velocity, steering and vibration behaviour [100]. Mostly, the longitudinal vehicle dynamics is considered to evaluate the performance of the EV powertrain in basic powertrain modelling [32], [101], [102]. The longitudinal vehicle dynamic sub-model is used for estimating the EV traction requirements by considering the input data of the vehicle and environmental conditions as exposed in Fig. 7.

The resistive forces considered for modelling are aerodynamic drag and road load (grading and rolling resistive force). The equations used for calculating the resistive and acceleration forces along with their influencing factors are discussed in Fig. 8. The F_t, T_t and P_t required at the wheel of EVs are calculated by using all the forces, effective wheel radius (R_w) and vehicle velocity (V_v) as described in equations 4, 5 and 6. During modelling, the numerical values of T_t and P_t are considered as a primary input to determine the size of the transmission, EM and power source.

$$F_t = F_{ae} + F_{ro} + F_g + F_{lac} \tag{4}$$

$$T_t = F_t * R_w \tag{5}$$

$$P_t = F_t * V_v \tag{6}$$

B. REGENERATIVE BRAKING

Unlike FVs, recovering kinetic energy during deceleration and braking is an added inherent feature in EVs which is achieved by the bi-directional functionality of electric drives [109]. During DC simulation, the total energy of the battery (E_{tot_bat}) is estimated by adding the magnitude of the integrated value of battery output (P_{bat_out}) and input power (P_{bat_in}) during traction and braking or deceleration [110] as stated in equation 7. Here, the (P_{bat_in}) sign is negative because of vehicle deceleration and negative grade angle (θ). According to equations 8 and 9, the input power to the battery from the regenerative braking system is estimated by using the regenerative braking factor (β), power at the wheel (P_{wheel_regen}) and powertrain efficiency ($\eta_{powertrain\_regen}$) during regenerative braking. Here,

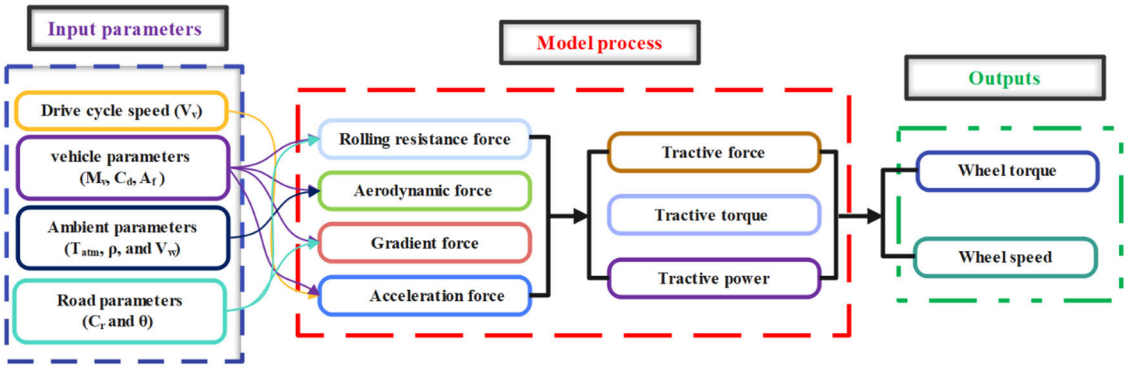

FIGURE 7. Longitudinal vehicle dynamic sub-model for estimating the EV traction requirements [103], [104], [105].

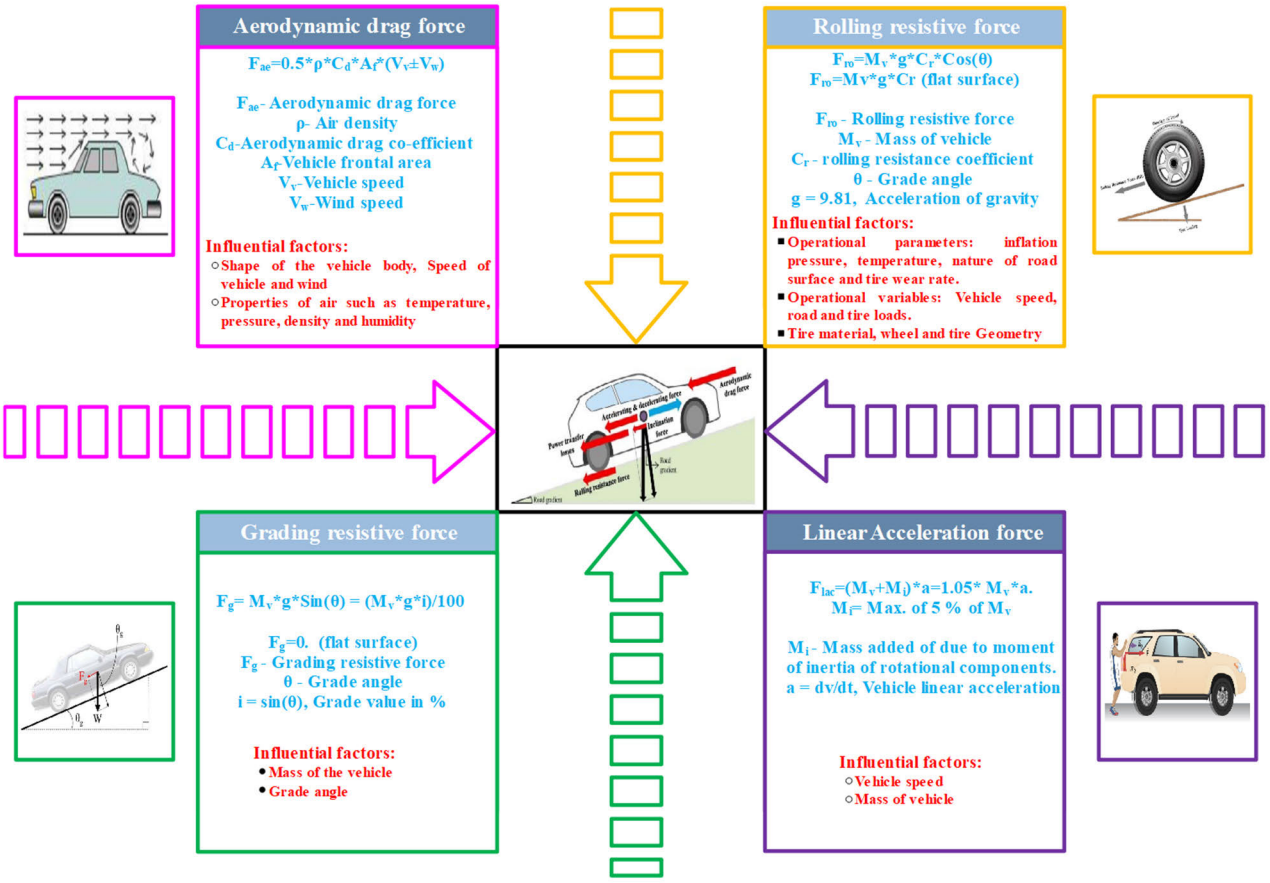

FIGURE 8. Schematic representation of equations used for calculating resistive and acceleration forces with influencing factors [106], [107], [108].

powertrain efficiency is assessed by multiplying the efficiency of transmission (η_{Trans}), electric drive ($\eta_{motordrive}$) and battery ($\eta_{battery}$) during the regenerative braking [111]. The value of β lies between 0 to 1 which expounds the amount of energy recovered from total brake energy by the traction motor [112]. In some cases, regenerative braking efficiency (η_{rb}) is used to denote the performance of regenerative braking that is delineated by the ratio of energy recovered ($E_{recoverable}$) and maximum available energy ($E_{available\_braking}$) at the wheel during braking [113]. Moreover, $E_{recoverable}$ to the battery is limited by the deceleration and braking force, V_v, G, adhesion coefficient of the tire, power source capability, maximum motor torque and efficiency of powertrain components [11], [34].

$$E_{tot\_bat} = \left(\int_{tr} P_{bat\_out}(t)\,dt - \int_{reg} P_{bat\_in}(t)\,dt \right) \quad (7)$$

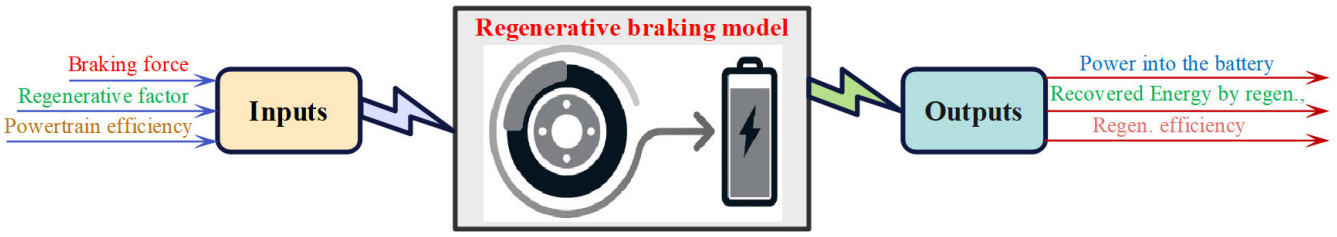

FIGURE 9. Outline of regenerative braking sub-model with its inputs and outputs.

$$P_{bat_{in}} = \beta * \frac{P_{wheel_{regen}}}{\left(\eta_{powertrain_{regen}}\right)} = \beta * \frac{(F_t * V_w)_{regen}}{\left(\eta_{battery} * \eta_{motordrive} * \eta_{Trans.}\right)_{regen}} \quad (8)$$

$$\eta_{rb} = \frac{E_{recoverable}}{E_{available\_braking}} \quad (9)$$

C. TIRE AND WHEEL

In most of the EV powertrain modelling studies, the tire and wheel sub-model is not considered as it has less impact on EV performance. However, it is essential to consider these sub-models for improving the accuracy of model outputs [114]. In real-time, the vehicle traction requirements differ from the modelling cases due to dynamic variation in wheel slip and rolling resistant co-efficient between tire and road surface at different driving and ambient conditions [115]. By considering the wheel slip, the total tractive power required for propelling the EV is defined as the addition of tractive power at the wheel (P_t) and power loss due to wheel slip (P_{slip}). Also, the P_{slip} between tire and wheel is calculated by multiplying the tangential force (maximum tractive force, F_z) and the difference in speed of wheel and vehicle (V_{slip}). Further, the magnitude of F_z is modelled with vertical tractive force on the wheel (F_t) and tractive effort co-efficient (μ) as given in equations from 10 to 12. Whereas the μ is a function of slippage value (S), which is significantly influenced by the inflation pressure of tire and road surfaces [105].

$$P_{total\_trac} = P_t + P_{slip} \quad (10)$$

$$P_{slip} = F_z * V_{slip} \quad (11)$$

$$F_Z = F_t * \mu(S) \quad (12)$$

Moreover, the maximum tractive force required on the wheel is closely related to the slip of the wheel, which is defined as the ratio of longitudinal velocity at the wheel and tire velocity at free rolling conditions. The equations for slip during traction (S_{tra}) and braking (S_{bra}) are given in equations 13 and 14. Here, ω_t and r_t are the angular speed and radius of the tire at free rolling. Also, the range of slip value is always positive between 0 to 1 at both conditions [116].

$$S_{tra} = \left(1 - \left({}^{V_w}/_{V_t}\right)\right) * 100 = \left(1 - \left({}^{V_w}/_{\omega_t * r_t}\right)\right) * 100 \quad (13)$$

$$S_{bra} = \left(1 - \left({}^{V_w}/_{V_t}\right)\right) * 100 = \left(1 - \left({}^{\omega_t * r_t}/_{V_w}\right)\right) * 100 \quad (14)$$

Apart from the wheel slip, the f_r is another key parameter of tire and road which is varied based on the material used, geometry, and nature of tire and road surface. However, the variation in f_r for different vehicle speeds should be considered for improving the accuracy of model output as stated in equation 15. which predicts the f_r with better accuracy when the vehicle speed is up to 128 km/h. [117].

$$f_r = 0.01\left(1 + {}^{V_w}/_{160}\right) \quad (15)$$

VI. MODELLING OF EV POWERTRAIN COMPONENTS

The modelling of powertrain components in EV comprises the sub-model of transmission, motor, power converter and battery. In this section, each sub-model is defined by a mathematical correlation with data sheet parameters to estimate the power output and losses along with their types and selection criteria as discussed below.

A. TRANSMISSION

Unlike FVs, the use of efficient power electronics-controlled EM in EVs replaces the multi-speed with gearless or single-speed gear transmission to match the wide ranges of EV tractive requirements [118]. However, a trade-off analysis between the size of EM and transmission is required to optimize the performance and cost of the drivetrain Also, it is essential to produce the maximum T_t at the same gear ratio (G) while the EV is climbing the road with higher grade [119]. The criteria for the gear ratio of transmission in EV is given in equation 16. Here T_m, $(\omega_m)_{max}$ and $(V_w)_{max}$ are motor torque, the maximum angular speed of the motor and wheel velocity [101].

$${}^{T_t}/_{(\eta_{Trans} * T_m)} \leq G \leq {}^{((\omega_m)_{max} * R_w * 2\Pi)}/_{((V_w)_{max} * 60)} \quad (16)$$

Through the transmission model, the motor torque T_m and speed (ω_m) can be found by the following equations 17-19 with the outputs from the vehicle dynamics model such as T_t, ω_w and η_{Trans} along with the constant value of G [120] as shown in Fig. 10.

$$T_m = {}^{T_t}/_{(G * \eta_{Trans})} \quad (17)$$

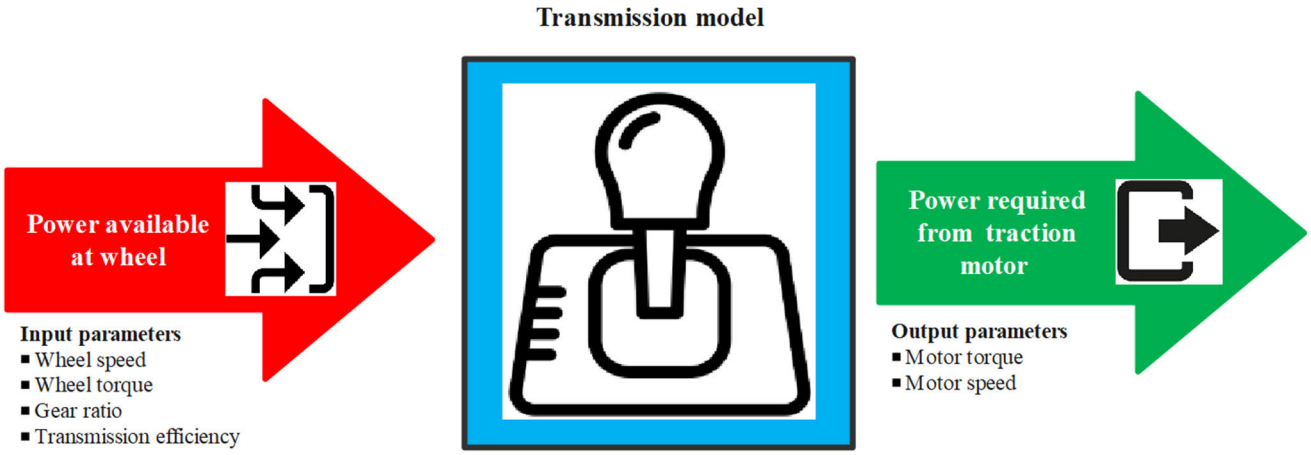

FIGURE 10. Outline of transmission sub-model with its inputs and outputs.

$$\omega_m = G * \omega_w \tag{18}$$

$$\omega_w = {V_w}/{R_w} \tag{19}$$

Here. ω_w and ω_m is the angular speed of the wheel and motor. Also, the efficiency of transmission during traction and regenerative braking [121] is defined by the following equations 20-21.

$$(\eta_{Trans})_{trac.} = {(T_w * \omega_w)}/{(T_m * \omega_m)} \tag{20}$$

$$(\eta_{Trans})_{regen.} = {(T_m * \omega_m)}/{(T_w * \omega_w)} \tag{21}$$

B. TRACTION MOTOR

The EV performance characteristics such as acceleration, passing ability, gradeability and maximum speed are steadfastly relying on the speed-torque and power characteristics of the EMs [122], [123]. The EM is selected by comparing their features such as starting Torque, power output, efficiency, ease of control, size, cost, noise, life and maintenance [124], [125]. The motor drive efficiency (η_{motor_drive}) is a key factor in evaluating the size of the power source, which is significantly affected by the efficiency of the power converter ($\eta_{pow.con}$) and EM (η_{motor}) [126], [127] as shown in equation 22.

$$\eta_{motor\_drive} = \eta_{motor} * \eta_{pow.con} \tag{22}$$

The studies based on evaluating the efficiency of different EMs are seeking much more attention towards researchers as it has lower efficiency with higher variability throughout operating regions than inverters [128]. Generally, the η_{motor} is obtained through a load test of EM coupled with a dynamometer. In some cases, the η_{motor} is obtained by the finite element method (FEM) through equivalent circuit parameters (ECP) such as data of geometry and material properties of specified motor [129]. Mostly, these data are not revealed by the manufacturer to the user. Also, the η_{motor}calculated from FEM is a higher time-consuming process and can provide accurate values when appropriate motor data is used [130]. The calculation of η_{motor} with its power components for BLDC motor [131], [132] is shown in below equations 23-24.

$$\begin{aligned}\eta_{motor} &= {P_{m.out}}/{P_{m.in}} = {P_{m.out}}/{(P_{m.out} + P_{loss})} \\ &= {(T_m * \omega_m)}/{((T_m * \omega_m) + P_{loss})}\end{aligned} \tag{23}$$

$$P_{loss} = Copper\ losses + Iron\ losses + mechanical\ losses \tag{24}$$

Here, $P_{m.in}$, $P_{m.out}$ and P_{loss} are motor power input, output and losses. The copper or ohmic losses are defined by the heat losses caused by the electrical resistance of wires, which are directly proportional to the current (I_m) and torque of the motor [133], [134] as shown in equation 25.

$$Copper\ losses = (I_m)^2 * R = K_c * (T_m)^2 \tag{25}$$

Here, R is the resistance and K_c is copper constant which is defined by magnetic flux and resistance of brushes and coil. Likewise, iron or core loss is another decisive factor in the calculation of η_{motor} which will be calculated by Steinmetz equations [135]. The iron losses are increased with an increase in the rate of magnetic field changes, which is directly proportional to the ω_m. Also, the core losses of EM are reduced with an increase in the operating temperature due to lower iron electric conductivity [136]. The iron losses are modelled with three sub-components such as eddy current (P_{eddy}), hysteresis (P_{hys}), and excess losses (P_{exc}) as presented [137] in the following equations 26-29.

$$Iron\ losses = P_{eddy} + P_{hys} + P_{exc} = K_i * \omega_m \tag{26}$$

$$P_{eddy} = K_{eddy} * f^2 * B^2 * V_{core} \tag{27}$$

$$P_{hys} = K_{hys} * f * B^2 * V_{core} \tag{28}$$

$$P_{exc} = K_{exc} * f^{1.5} * B^{1.5} * V_{core} \tag{29}$$

where K_i is the current constant which is defined by the way the magnetic field is induced in the motor. K_{eddy}, K_{hys} and K_{exc} are steinmetz eddy current, hysteresis and excess

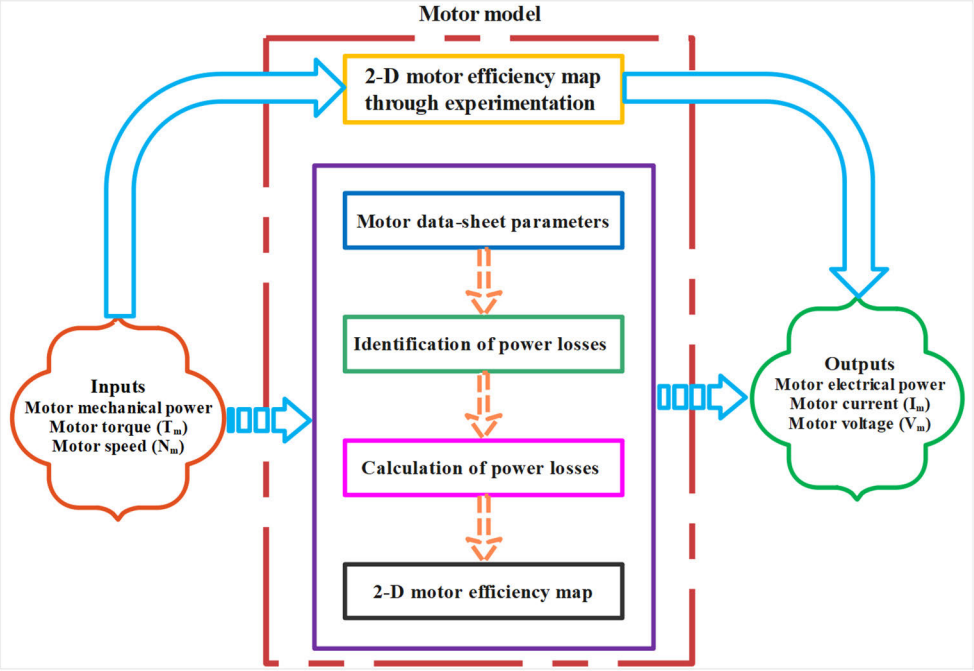

FIGURE 11. Overview on the function of motor sub-model.

losses constant which differ based on the types of lamination material used in the rotor and stator. The V_{core}, B and "f" are iron core volume, flux density and frequency of changes in the magnetic field [138], [139]. Similarly, mechanical losses are another component of motor losses, which comprises friction and windage losses as seen in equation 30. It is subjected to vary by motor speeds not by the type of power supply.

$$\begin{aligned} Mechanical\ losses &= Friction\ and\ windage\ losses \\ &= C + (K_w * (\omega_m)^3 \end{aligned} \tag{30}$$

Similarly, the losses in IM and PMs are varied based on the number of stators and rotors in the motor, air resistance and friction in the bearing [140], [141]. The power losses in IM and PM are defined in terms of T^m and ω^n [128] as shown in equation 31.

$$P_{loss}\,(T,\omega) = \sum K_{mn} T^m \omega^n \tag{31}$$

Here, m, n and K_{mn} are integers and constants which are varied based on the operating regions of the motor such as constant torque and power regions. Along with the copper and iron losses, stray loss (P_s) is additionally considered for IMs, which is complex and very difficult to calculate. It comprises several sub-component losses such as cross-path, surface (P_{sur}), pulsation (P_t), rotor harmonic current (P_B) and flux leakage losses [142], [143]. Almost, 2% of power from the rated-power capacity of IM is lost as stray losses. Mostly, the cross-path and flex leakage losses have been very low in recent days due to the advanced design features of IM. Equations 32 and 33 are defined as the stary loss, which is in proportion to the square of the stator current (I_I) [144], [145].

$$P_{sur} \propto I_I^2 f_I^{1.5};\ P_t \propto I_I^2;\ P_B \propto I_I^2 \tag{32}$$

$$P_s = P_{sur} + P_t + P_B = 0.01 * P_{2N} * \left(\frac{I_I}{I_{IN}}\right)^2 * \left[\left(\frac{f_I}{f_{IN}}\right)^2 + 1\right] \tag{33}$$

where I_{IN}, f_{IN} and P_{2N} are rated current, frequency and power of IMs. Through the motor sub-model, the $P_{m.in}$ can be calculated as shown in Fig. 11 with the value of $P_{m.out}$ from the transmission model and η_{motor} which is calculated from the datasheet parameters of EM. Further, the I_m is calculated from the motor voltage for the entire DCs.

C. POWER CONVERTER

The DC-AC inverter and DC-DC converter are the most common types of power converters used in electric powertrains to regulate the current and voltage at the required magnitude and form [146]. Fig. 12. elaborates on the power flow and estimation of losses through data sheet parameters in the power converter during modelling.

1) DC-AC INVERTER

Particularly, a bi-directional inverter with an appropriate power rating is used in between the prime mover and battery of EVs to convert the DC into AC at the required magnitude and frequency. In recent days, more research has focused on the usage of inverters fabricated by silicon carbide metal–oxide semiconductor field-effect transistors

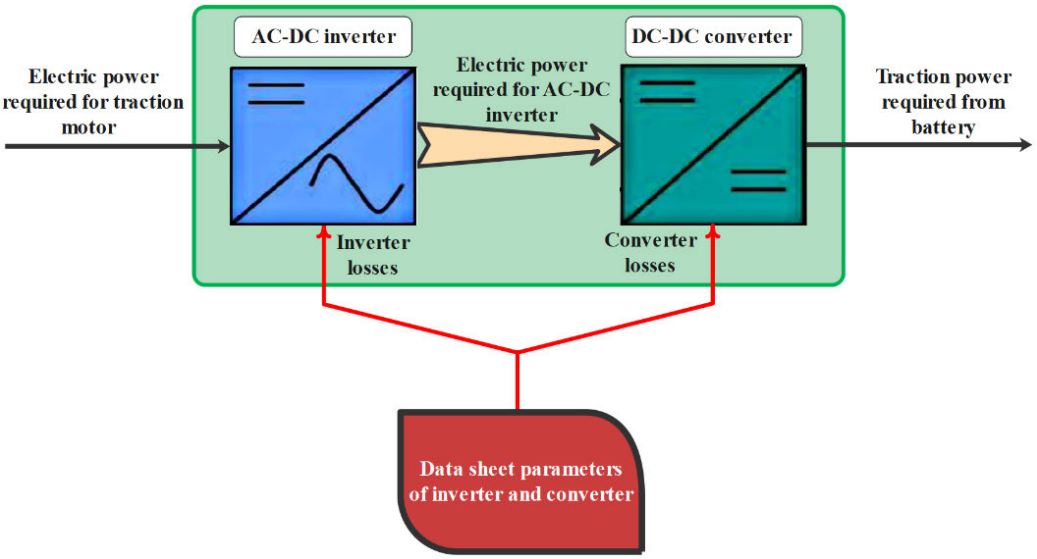

FIGURE 12. Schematic representation of Power flow in power converter sub-model.

(SiC MOSFET) with freewheeling diode than silicon-based power converters and insulated-gate bipolar transistor (Si IGBT) [147]. This can be justified by a wide energy band gap, higher efficiency, power density, thermal conductivity and switching speed of SiC MOSFET. The efficiency of the inverter (η_{inv}) is defined by the ratio of motor input power ($P_{m.in}$) and battery output power (P_{o/p_bat}) as seen in equation 34, which is an influential parameter to define the size of the battery in EVs [148].

$$\eta_{inv} = \frac{P_{m.in}}{P_{o/p\_bat}} = \frac{P_{m.in}}{P_{m.in} + P_{lo\_inv}} \tag{34}$$

Here, P_{lo_inv} denotes the losses in the inverter, which encompasses switching and conduction losses of IGBT or MOSFET power switches and diodes. Further, it varies significantly according to hardware parameters and operating conditions like gate driver resistance, materials and coolant used, motor power factor, switching frequency, temperature, pulse width modulation (PWM) strategy, T_m and ω_m [149], [150]. In most cases, the P_{lo_inv} and η_{inv} are evaluated and mapped through the electro-thermal analysis by using static and dynamic parameters. In some studies, blanking time, reverse conduction and the thermal impedance between power switches and cooling systems at a transient state are considered to improve the accuracy of η_{inv} [149], [151]. Also, the performance of the inverter is analyzed by using the quality factor matrix (Q) with DC simulation as given in equation 35, which decides the size of the thermal management system required [152].

$$Q = \frac{\int |P_{m.in}|\, dt}{\int P_{lo\_inv} dt} \tag{35}$$

As seen in equation 36, the power losses in Si IGBT-based inverter ($P_{loss\_IGBT\_Inv}$) are defined by including the conduction (P_{con_IGBT} and P_{con_d}) and switching losses (P_{sw_IGBT} and P_{sw_d}) of IGBT power switches and freewheeling diodes. Also, the $P_{loss\_IGBT\_Inv}$ is varied based on the number of IGBTs (N_{IGBT}) and diodes (N_D) used in the inverter according to the current rating [153]. Subsequently, different components of power losses for Si IGBT-based inverters are given in equations 36-40.

$$P_{loss\_IGBT\_Inv} = N_{IGBT}\left(P_{con\_IGBT} + P_{sw\_IGBT}\right) + N_D\left(P_{con\_d} + P_{sw\_d}\right) \tag{36}$$

$$P_{con\_IGBT} = V_{CE\_0} I_{I\_avg} + R_{CE} I^2_{I\_rms} \tag{37}$$

$$P_{sw\_IGBT} = \left(E_{I\_on} + E_{I\_off}\right) f_s \tag{38}$$

$$P_{con\_d} = V_F I_{D\_avg} + R_d I^2_{D\_rms} \tag{39}$$

$$P_{sw_d} = (Q_{rr} V_d) f_s \tag{40}$$

Here, V_{CE_0} and R_{CE} are saturation voltage and ohmic resistance. I_{I_rms} and I_{I_avg} are the root mean square (RMS) and the average of the collector current. E_{I_off} and E_{I_on} are energy losses during switch on and off operation. f_s, V_F and R_d are the switching frequency, threshold voltage and direct resistance. I_{D_avg} and I_{D_rms} are the average and RMS of the current flowing through the diode. Q_{rr} is the reverse recovery charge, V_d is the voltage across the diode during reverse recovery. Like IGBT-based inverters, power losses of MOSFET-based inverters can be modelled by using equations 41-44. In the case of MOSFET, the conduction losses in diodes are not considered as it is very low in magnitude [154], [155].

$$P_{loss\_MOSFET\_Inv} = N_{MOSFET}\left(P_{con\_M} + P_{sw\_M}\right) + N_D\left(P_{sw\_d}\right) \tag{41}$$

$$P_{con\_M} = R_{ds\_on} I^2_{M\_rms} \tag{42}$$

$$P_{sw\_M} = \left(E_{M\_on} + E_{M\_off}\right) f_s \tag{43}$$

$$P_{sw\_d} = (Q_{rr} V_d) f_s \tag{44}$$

Here, R_{ds_on} is the on-resistance and I_{M_rms} is the RMS drain current. For both types of inverters, power losses due to conduction depend on the I_{rms} which is higher at the high torque operating region of the motor. Also, the switching losses in the inverters are influenced by the switching frequency and speed of the motor. From several studies, it can be concluded that the SiC MOSFET-based inverters are outperformed at higher switching frequencies and constant torque regions than Si IGBT-based inverters due to their reverse conduction potential [155], [156].

2) DC-DC CONVERTER

During traction and regeneration, the bi-directional DC-DC converter is used for interfacing power sources with traction drive and auxiliary devices by decrementing or boosting the voltage [157]. Though the output voltage of the battery varies with SOC, the DC-DC converter is designed to integrate the battery and high-voltage DC-link [158]. The DC-DC converter is classified based on the frequency and isolation requirement such as non-isolated (low-frequency) and isolated converters (high-frequency) [159], [160]. In several studies, the efficiency of DC-DC converters (η_{conv}) is also considered to predict the battery size accurately [161]. The η_{conv} is defined by the ratio of input power to DC-link or inverter (P_{i/p_inv}) and battery output power (P_{o/p_bat}) as stated in equations 45 and 46.

$$\eta_{con} = \frac{P_{i/p\_inv}}{P_{o/p\_bat}} = \frac{P_{o/p\_bat} - \sum P_{loss\_conv}}{P_{o/p\_bat}} \tag{45}$$

$$\sum P_{loss_{conv}} = P_{con_{IGBT}} + P_{sw_{IGBT}} + P_{con_d} + P_{sw_d} + P_{cap} + P_{core} + P_{cop} \tag{46}$$

Other than switching and diode losses in DC-DC converters, the total power loss of the converter (P_{loss_conv}) includes capacitor (P_{cap}), inductor's core (P_{I_Core}) and copper (P_{I_Cop}) losses as given in equations 46-48.

$$P_{Cap} = R_C I^2_{C\_rms} \tag{47}$$

$$P_{I\_Cop} = R_I I^2_{I\_rms} \tag{48}$$

$$P_{I\_Core} = W_C P_C \tag{49}$$

Here, the P_{cap} is dependent on the resistance (R_C) and RMS current value (I_{C_rms}) of capacitors which are highly influenced by the selection of capacitors for DC-DC converters in EV applications. Similarly, the inductors for converters are selected by the trade-off between the value of its copper and core losses [158], [162]. Further, the (P_{I_Cop}) is reliable on the resistance (R_I) and RMS current value (I_{I_rms}) of the inductor. Also, the P_{I_Core} is evaluated by multiplying the core weight (W_C) and iron losses per Kg (P_C) which is quantified by phenomena of eddy current and hysteresis losses due to different mechanisms involved in the magnetic field fluctuations [163]. In EVs, the low-voltage DC power is magnified into high-voltage DC power and supplied to the inverter with a converter efficiency range of 90-95% [164], [165].

D. BATTERY

Among the various energy sources, secondary batteries i.e., rechargeable batteries are most suitable for EV applications due to their superior performance and smooth operation [166]. Predominantly, the lithium-ion battery is employed as an energy source in EVs as it has inimitable features such as high voltage potential, lightweight, and high energy density with low-self discharge [167]. The EC, DR and other outputs of the battery sub-model are represented in Fig.13. along with inputs required such as total power required from the battery voltage.

1) BATTERY AND CHARGER POWER

The total power required from a battery pack (P_{Bat}) is estimated by the power consumed by the auxiliary systems ($P_{aux.sys}$), $P_{m.in}$, η_{inv} and η_{con} as shown in equation 49. Also, the output power of the battery during traction (P_{o/p_bat}) is stated by multiplying the output voltage ($V_{Bat\_0/p}$) and current of the battery ($I_{\_bat}$) [120] in the subsequent equation 50.

$$P_{Bat} = \left(\frac{P_{m.in}}{(\eta_{invertor} * \eta_{converter})}\right) + P_{aux.sys} \tag{50}$$

$$P_{o/p\_bat} = V_{Bat\_0/p} * I_{bat} \tag{51}$$

In most cases, the value of $P_{aux.sys}$ is considered as the maximum power consumed by the auxiliary systems such as air conditioning, electrical steering, light systems, infotainment systems, controllers, etc. However, the recommended usage power capacity of the battery by the manufacturer is approximately 80-85% of the actual power to prolong the battery life [168], [169]. Also, the power of the charger ($P_{charger}$) is estimated by the ratio of P_{bat} and the time required for full charging (t_{ch}) as given in equation 51. Also, the current rating of the charger ($I_{charger}$) is modelled based on the $P_{charger}$ and V_{bat} of the battery [170] as seen in equation 52.

$$P_{charger} = \frac{P_{bat}}{t_{ch}} \tag{52}$$

$$I_{charger} = \frac{P_{charger}}{V_{bat}} \tag{53}$$

2) BATTERY ENERGY

The battery energy consumption acts as an indicator of how efficiently energy is converted through the powertrain components of EVs. The required battery energy (E_{Bat}) of EVs is estimated by integrating the battery power (P_{Bat}) as stated in equation 53. The total battery energy required per km ($B.E_{Km}$) is calculated by using E_{Bat} and DC distance. With E_{Bat}, the DR of the EV is estimated with the total battery energy ($T.E_{Bat}$) [171] as stated in equations 54 and 55.

$$E_{Bat} = \int P_{Bat} dt \tag{54}$$

$$B.E_{Km} = \left(\frac{E_{Bat}}{(3.6 * 10^3 * Drive\ cycle\ distance)}\right) \tag{55}$$

$$(DR)_{Desired} = T.E_{Bat}/B.E_{Km} \tag{56}$$

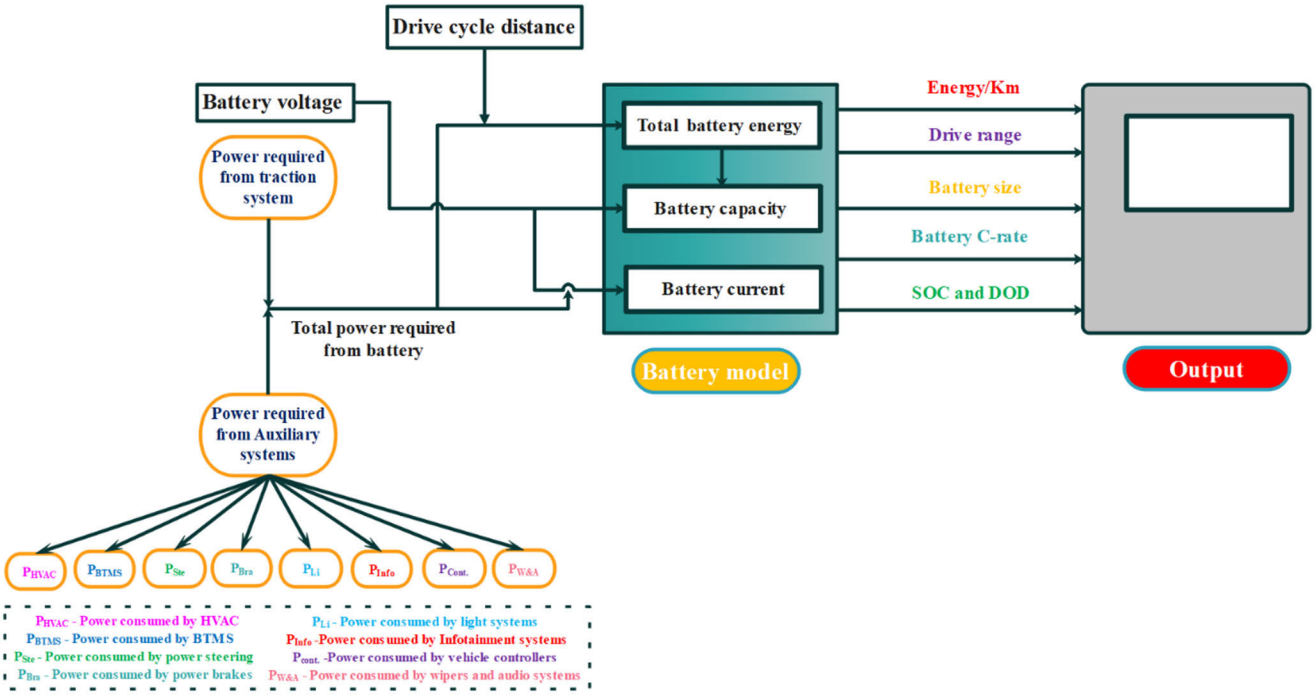

FIGURE 13. Outline of battery sub-model with its inputs and outputs.

3) BATTERY CAPACITY OR RATINGS AND SIZE

The battery pack rating is the most vital parameter of a power source which influences the weight, DR and cost of the vehicle. The total current capacity of the battery (C_{Bat}) is calculated by using the $T.E_{Bat}$ and V_{Bat} as given in equation 56.

$$C_{Bat} = \frac{T.E_{Bat}}{V_{Bat}} \tag{57}$$

Based on the requirement of battery capacity and voltage in EVs, the number of cells arranged in series (N_S) and parallel (N_p) in the battery are defined by using equations 57 and 58. Also, the arrangements of cells in a battery pack should meet the requirement of mechanical, thermal and electrical design considerations [172], [173].

$$N_S = \frac{V_{Bat}}{V_{Cell}} \tag{58}$$

$$N_p = \frac{C_{Bat}}{C_{Cell}} \tag{59}$$

Here, V_{Cell} and C_{Cel}l are cell voltage and current capacity.

4) BATTERY CURRENT AND VOLTAGE

The amount of current supplied by the battery or flow into the battery is based on the battery capacity, the power requirement of EM and the efficiency of regenerative braking [174]. Further, the amount of current drawn from the battery during traction and supplied to the battery during regeneration is defined by equations 59 and 60. The battery C-rate is characterized based on the amount of current discharged and charged during traction and regeneration or charging [175], [176] as shown in equation 61.

$$I_{bat\_Trac} = \frac{V_{OC} - \sqrt{V_{OC}^2 - 4R_i P_{bat}}}{2R_i} \tag{60}$$

$$I_{bat\_Regen} = \frac{-V_{OC} + \sqrt{V_{OC}^2 + 4R_i P_{bat}}}{2R_i} \tag{61}$$

$$\text{Battery C-rate} = \frac{I_{ch} or I_{disch}}{C_{bat}} \tag{62}$$

Here, I_{ch} or I_{disch}, $R_i$and V_{OC} are the charge or discharge current, internal resistance and open circuit voltage. Also, the amount of current supplied to the auxiliary systems ($I_{aux.sys}$) is calculated [26] using equation 62.

$$I_{aux.sys} = \left(\frac{P_{aux.sys}}{(\mathbf{V}_{bat} * \boldsymbol{\eta}_{conv})} \right) \tag{63}$$

Also, the $V_{Bat\_0/p}$ depends on the Coulombic Efficiency (η_{cl}) of the battery as given in equation 63. Normally, η_cl is about 100 % for Li-ion batteries [106], [177].

5) BATTERY SOC

The SOC of the battery designates the amount of charge capacity in the battery, which is normally defined by the range of 0 to 100%. Also, it is recommended by the manufacturer to maintain the battery SOC from 10 to 90 % to ensure better battery performance [178]. As shown in equation 64, the SOC of the battery at the moment (SOC(t)) is calculated by using an equivalent circuit model based on the ratio of

current battery capacity (C_{bat}) and maximum battery capacity (C_{max}). Also, the sign is negative during traction and positive during regeneration and charging [179]. Further, the depth-of-discharge (DOD) is estimated based on SOC(t) as shown in equation 65.

$$SOC\,(t) = 1 - \left({}^{C_{bat}}/_{C_{max}}\right) = SOC_i \pm \left[\left({}^{1}/_{3600 * C_{bat}}\right) * \int_0^t I_{bat}\,dt\right] \quad (64)$$

$$\mathrm{DOD} = 1 - SOC\,(t) \quad (65)$$

Here, SOC_i is the initial SOC of the battery. Also, the V_{Bat} varies with the amount of I_{bat} and SOC. Through the above equations in the battery sub-model, the maximum required battery capacity and power, cell configuration, DR and charger rating can be calculated throughout the DC duration. Also, dynamic parameters of batteries such as battery current, voltage, SOC and DOD are calculated during different driving conditions.

VII. SIMULATION PROCESS AND TOOLS USED TO ESTIMATE THE EV POWERTRAIN PERFORMANCE CHARACTERISTICS

Most commonly, the performance of the EV powertrain is demarcated by the EC and DR [180], [181], [182]. Also, powertrain operating regions or efficiency, EV acceleration and gradeability performances need to be cautiously considered to evaluate the capability of powertrain components [183], [184]. During the design and development process of the EV powertrain, simulation is the most essential process to meet the trustworthy or effective system-level design. Initially, the simulation process of the EV powertrain involves the collection of data related to DC, vehicle dynamic and datasheet parameters, efficiency map and ambient conditions [185]. Further, the simulation can be done with the existing EV model in the simulation tools, which has all the sub-models associated with the appropriate mathematical equations to evaluate the performance of EVs as discussed in sections V to VIII. In certain cases, the model is customized according to the variations in powertrain configurations and input parameters. Further, these tools are focused on evaluating the different performance features of EVs such as EC and DR, powertrain capability, and integration of EVs with grid systems under different scenarios [186]. The simulation tools are chosen based on certain criteria like ability to customize the model, accuracy, user-friendliness, time consumption and system requirements. As this review article is intended to guide the researchers towards an estimation of EC, DR and other powertrain performance parameters of EVs. The most common simulation tool used for evaluating the aforementioned parameters is Simulink with MATLAB [96], [174], [187], [188], [189], [190], [191], [192]. Other than this, there are several tools used to evaluate the EV powertrain performance which are elaborated in Fig. 14 with its key features, merits and demerits [193].

VIII. EFFECT OF DIFFERENT INPUT VARIABLES ON EV POWERTRAIN PERFORMANCE

The influential parameters on EV performances are categorized into internal and external factors as shown in Fig. 15. Further, Table. 2. elaborates on the simulation studies based on the estimation of performance factors for electric-2-wheelers (E2W) and electric-3-wheelers (E3W) at different DCs. Mostly, IDC is used as a DC for evaluating performance other than WLTC, NEDC, etc. Similarly, simulation is done for electric-4-wheelers (E4W) in most cases with standard DCs such as NEDC, WLTC, HWEFT, FTP, EPA, etc., Table 3 reviews the simulation studies carried out for E4Ws to evaluate the EC and DR. The effect of influential variables or parameters on different EV performance aspects (EC and DR, acceleration and gradeability, powertrain efficiency, maximum vehicle torque and power) is illustrated in Fig. 16 and discussed from different simulation studies below.

A. ENERGY CONSUMPTION AND DRIVING RANGE

The key performance characteristics such as EC and DR have given a clear indication of EV on-road performance to the user. From simulation studies, it is evident that vehicle-related parameters such as M_v, f_r, C_d, A_f and $P_{aux.sys}$ are primarily impacting the EC of EVs [211]. Moreover, an increase in M_v significantly shows a negative trend on the EC and DR as it notably increases the rolling resistive force (F_{ro}) of EVs and leads to inefficient operating regions of powertrain components. Also, the DR is reduced as an increase in M_v leads to lower regeneration capability because of the increase in the usage of mechanical brakes [212]. Similarly, aerodynamic force parameters related to the vehicle like C_d and A_f have significantly affected the EC and DR at high speeds than low speeds [213]. Further, the design of these parameters plays a vital role when increasing the DR of EVs on highways where they travel at maximum speed. Contrary, an increase in f_r with inappropriate tire size or material used and a slippery road surface causes higher EC as the vehicle requires more T_t during low-speed conditions [37]. Further, an increase in $P_{aux.sys}$, frequent acceleration and deceleration leads to higher total EC with a lesser DR because of the inefficient operating conditions and higher power losses in EV powertrain [214].

The size and speciation of powertrain components in EVs influence the EC and DR significantly. The use of lower energy and power density battery and motor in the EV results in a lower DR with the same vehicle specification. Also, the increased size of drivetrain components increases the M_v and results in higher energy required to overcome the large resistive force [215]. Further, the use of multi-speed and continuously variable transmission (CVT) affects EC and DR as it has lower efficiency and higher transmission losses [216]. Like the vehicle parameters, atmosphere and driving conditions such as air temperature, density, road topography and driving behaviour have influenced the EC and DR at simulation and real-time testing. Moreover, the low atmospheric temperature with higher humidity and density of air increases

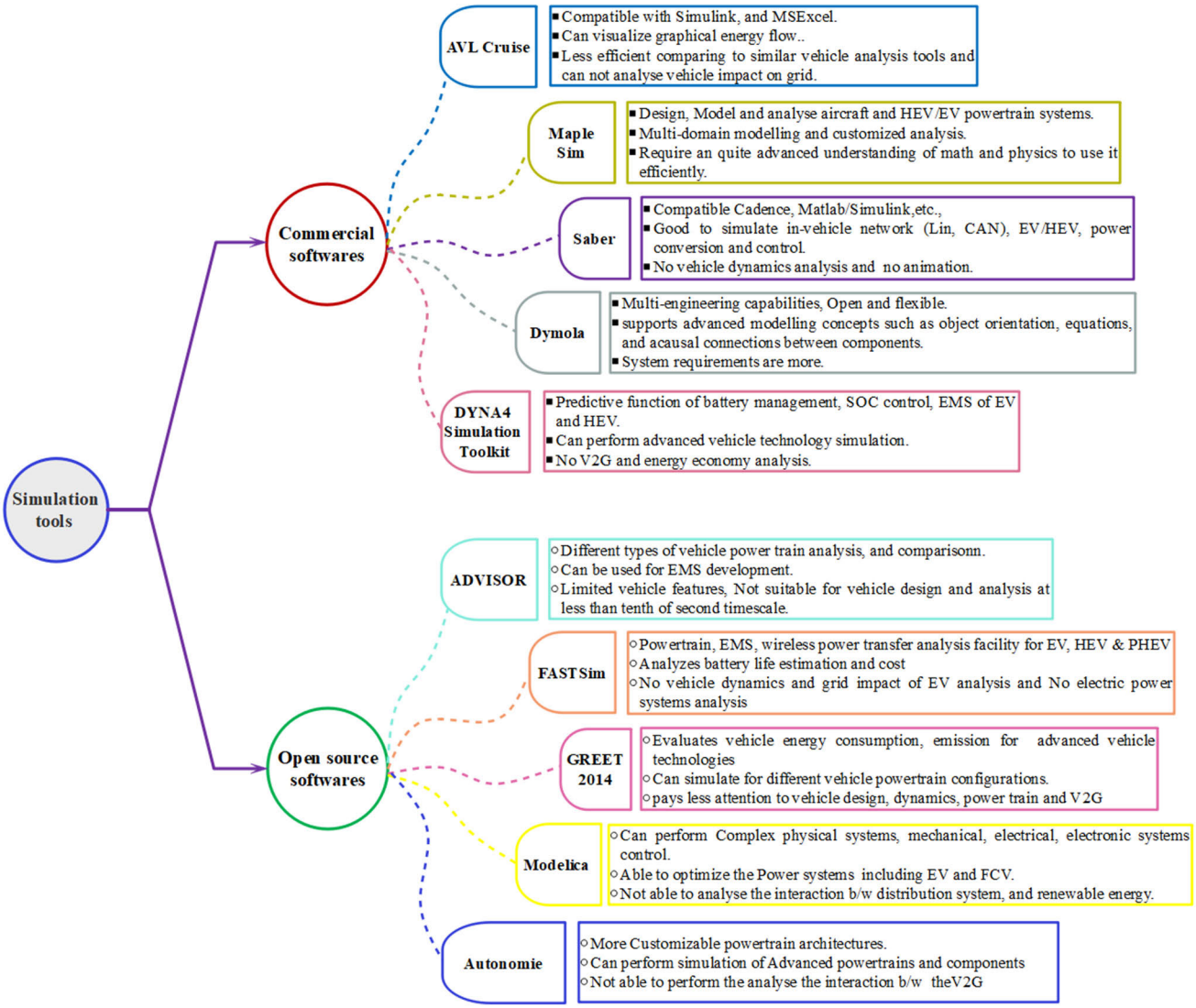

FIGURE 14. Features, merits and demerits of simulation tools used for EV energy consumption estimation.

the EC of EVs. Thus, $P_{aux.sys}$ is increased for improving the battery performance, cabin comfort and drivability. Also, the energy required to overcome the f_r and C_d is predominantly higher at the above-mentioned atmosphere conditions and results in lower DR of EVs [217], [218]. Likewise, an increase in headwind consequences higher EC at high speeds in motorways and reduces the DR of EVs. In fact, road surfaces with a higher slope require higher torque at the wheel to overcome the F_{gr}. In such cases, battery energy reduces rapidly with the supply of higher I_{bat} which results in lower DR [219]. As well, driving modes like eco and aggressive play a critical role in EC and DR based on vehicle speeds. The eco-driving mode at low speeds in urban causes higher EC due to long travel time. Meanwhile, the aggressive driving mode at high speeds on the motorway causes higher EC with the greater influence of aerodynamic resistive force on EVs [220].

B. ACCELERATION AND GRADEABILITY

The tractive capability, vehicle longitudinal performance, and ability of interaction between tire and road surface are well-defined with acceleration and gradeability performance of EV which are quantified with the tractive torque available in the wheel during the acceleration and climbing uphill. Several factors related to vehicle and road conditions have a greater influence on the acceleration and gradeability of EVs. An increase in M_v extremely limits the capability of acceleration and gradeability owing to the requirement for higher F_t at lower speeds [221]. Also, the decrease in acceleration and gradeability performance is found with an increase of f_r between tire and road surface due to a slippery surface and high friction coefficient. Similarly, the increase in $P_{aux.sys}$ reduces the power share of powertrain components from the battery which is reflected in the tractive torque available on

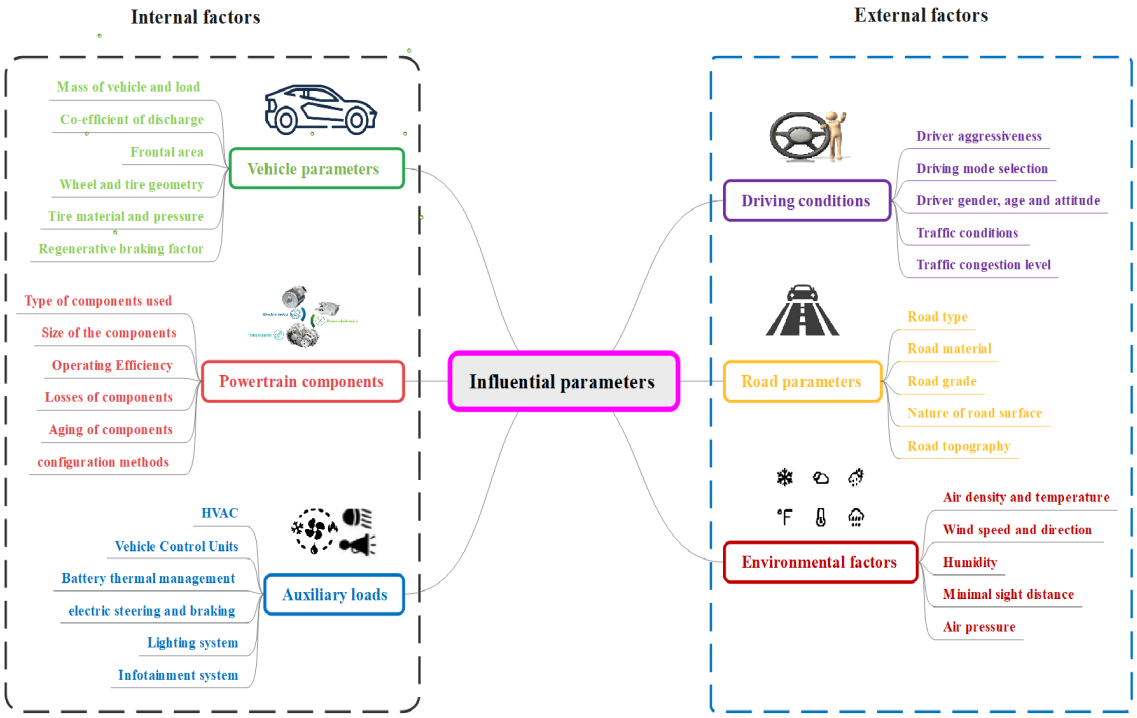

FIGURE 15. Different internal and external factors affecting EV energy consumption [37], [194], [195].

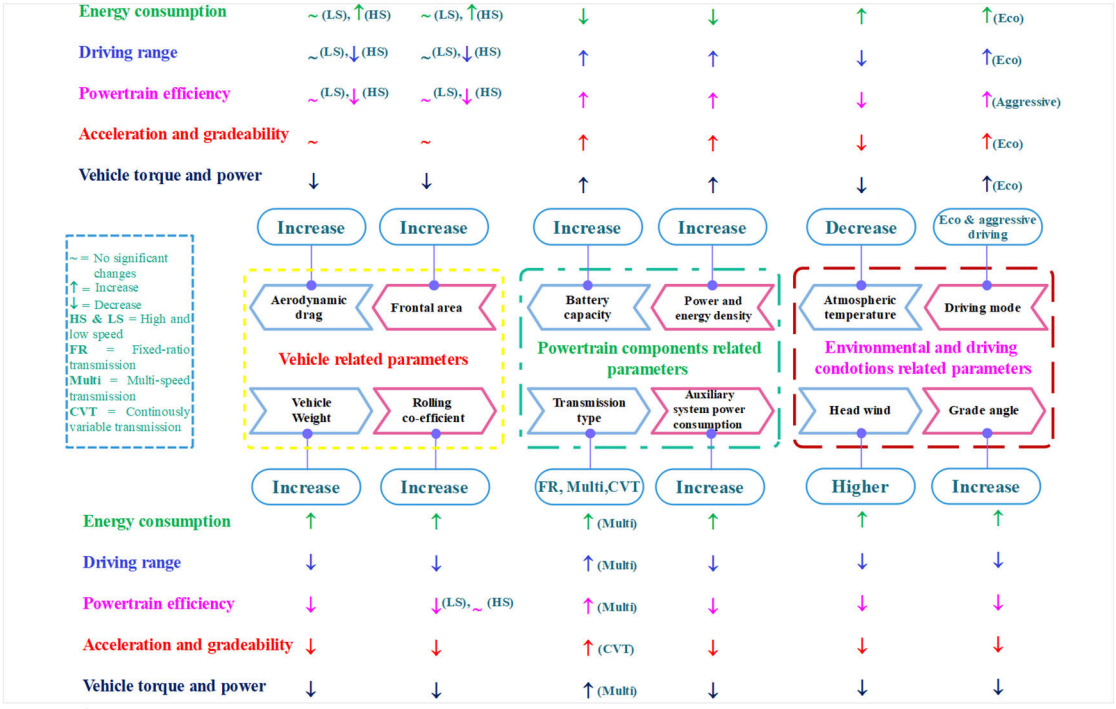

FIGURE 16. Effect of influential parameters on EV performance characteristics.

the wheel and results in an extension of the acceleration duration along with lower gradeability.

Moreover, an increase in battery size increases the capability of acceleration and climbing uphill as it provides more energy and power to the drivetrain components. Particularly, the inertia mass is increased with an increase in the size of drivetrain components such as the motor and transmission which extends the acceleration time and limits the maximum acceleration and gradeability [222]. Though the use of single-speed transmission with higher G and

TABLE 2. Drive cycle performance simulation studies on different E2W and E3W configurations.

Ref.	Vehicle type	Driving cycle	Vehicle specifications					Battery specifications and auxiliary load				Motor specifications				Transmission specifications			EV performance indicators				
			M_V (Kg)	C_d	A_f (m^2)	C_r	R_w (m)	Type	Capacity	N.V (V)	P_{aux} (W)	Type	P_{rat}/ P_{max} (Kw)	T_{rat}/ T_{max} (Nm)	η_m (%)	Type	T.R	η_t (%)	Vehicle range (Km)	E_{km} (Wh)	Acceleration performance (Kmh@sec)	Gradeability performance	Maximum speed (Km/hr)
[113]	E2W	ISO 13064-1:2012	250	0.6	0.8	0.013	*0.26*	Li-ion	3 kwh	115	100	BLDC	3/5	20/25	2-D map	Fixed	01:06	_	60.46	56	60@5	20deg	110
[196]		IDC	140	1.1	0.52	0.015	0.22	Li-ion, UC	41.4 Wh	38, 32	_	_	2	_	85	_	_	_	12	_	_	4%	42
[197]		WLTC	186	_	_	_	0.22	Li-ion	_	60	_	BLDC	_	_	_	_	_	_	120	35.26	_	_	
[198]		NEDC	282	0.7	0.36	0.007	0.20	Li-ion	2.6 kWh	_	_	_	_	_	_	Fixed	10	90	95	20.24	_	_	
		IDC																	130	27.79			
[199]		UDDS	250	0.6	0.8	0.013	*0.26*	Li-ion	3 kwh	100	100		3.5	27	95		01:05	_	70	25.74	_	_	128
[200]		ECE-47	195, 270	0.9	0.6	0.014	_	Li-ion, UC	32 Ah, 170 F	47, 27	60	BLDC	_/3 & 3.75	55/59	80			80	51.7, 66	_	_	_	-
[201]			798					Lead acid	180 Ah	48	_	BLDC	5.8	46	85	Fixed	4.1	97.5	70	52	_	_	-
			550					Li-ion	80Ah	48			4.24	36						44.08			
[202]	E3W	IDC	965	0.44	2.09	0.015	*0.22*	Li-ion	144 Ah	50	_	PMSM	_/7	_/42		_	_	_	105	_	_	18%	
[203]			678					Li-ion, UC	73 kWh, 1200 F	48, 32	_	BLDC	5.5/-	14.5	85	_	_	_	60	65.83	_	19% @15 km/hr	42
[204]			800	0.34	2.22	0.018	0.23	_	_	_	_	_	3.5/7	_	85	Fixed	_	90	100	_	_	0-15 deg	

TABLE 3. Drive cycle performance simulation studies on different E4W configurations.

Ref.	Driving cycle	Vehicle specifications					Battery specifications and auxiliary load				Motor specifications				Transmission specifications			EV performance indicators			
		M_V (Kg)	C_d	A_f (m^2)	C_r	R_w (m)	Type	Capacity	N.V (V)	P_{aux} (W)	Type	P_{rat}/ P_{max} (Kw)	T_{rat}/ T_{max} (Nm)	η_m (%)	Type	T.R	η_t (%)	Vehicle range (Km)	E_{km} (Wh)	Acceleration performance (Kmh@sec)	Gradeability performance
[205]	NEDC	1420	0.3	2.38	_	*0.36*		22 kWh	355.2	1800	PMSM	_/125	_/250	2-D map	Fixed	9.7:1	97	170	143	100@7.9	
	EPA																	115	176		
[45]	NEDC	1800	0.4	2	0.015	_		66 Ah	320	_	PMSM	30	100/ 200	2-D map	_	_	90	_	172	_	_
[72]	WLTC	1650	0.28	2.74	0.012			21.3 kWh	_	2000	_	_/80	_/254	2-D map	Fixed	7.9:1	85-95	202..33	105	_	_
	NEDC																	136	156		
[206]	FTP 72 HWFET JA1015	1400	0.284	1.97	0.015	0.30	Li-ion	160 Ah	312	_	PMSM	28/70	90/223	_	_	_	_	227.53 204.16 236.69	_	100@11.91	35.5% @ 30 km/hr
[207]	UDDS HWFET UDDS HWFET	1780	0.28	2.2	0.016	0.32		26	360	_	_	40/75	135/ 250	79 86 80.2 87.2	Fixed Two-speed	6.82:1 11.4, 4.64	-	142.1 157.7 130.4 141.8	-	100@13.48 100@13.49	25% 45%
[208]	NEDC Chinese Urban	1350	0.284	0.97	0.018	0.28		18 kWh	320	_	_	30/40	-	75-89 76-86			90	100 110	15.29 12.48	50@5.7	20.70%
[209]	EPA 75 HWFET EPA 75 HWFET	1807	0.359	3.2	_	0.31	_	28 kWh	_	_	IM	65/100	158/ 314	2-D map	Fixed Two-speed	9.3:1 9, 17	98 95	-	177.5 211.9 171.1 210.4	-	40.60% 70%
[97]	UDDS	1700	0.26	2.42	0.013	0.23		23 kWh	350	_	_	_/107	_/250	2-D map	Fixed	7.82:1	_	_	184.23	_	_
[210]	NEDC WLTC RDC	1000, 1500, 2000	_	_	_	_	Li-ion	25 kWh	360	_	Asynchronous	_	240/_	2-D map	Fixed	6.058	_	_	101-135 130-150 125-162		
[121]	WLTC-Class 3 NEDC FTP—75 WLTC-Class 3 NEDC FTP—75	1645	0.28	2.19	0.008	0.31	_	_	_	300	_	_/80	_/280	97%	Fixed Two-speed	8.19 9.27, 4.5	95	-	136 129 126 132 126 123	100@11.5 _	-

multi-speed transmission increases the M_v, the acceleration and gradeability performance is better than fixed single-speed transmission due to the extensive range of vehicle load [223]. Climatic conditions such as low atmosphere temperature with higher humidity and headwind prominently affect the acceleration and gradeability performance. Also, it minimizes the capability of the maximum acceleration and gradeability of the EVs as it increases f_r and wheel slip with the above-stated climatic conditions in most of the simulation studies. Similarly, the gradeability and maximum acceleration of EV are suppressed with higher θ due to the requirement of higher torque than flat road surface [224].

C. POWERTRAIN EFFICIENCY

In the simulation studies, the powertrain efficiency ($\eta_{powertrain}$) of the EV has purely relied on the operating region of powertrain components, torque and power requirement at the wheel [225]. Moreover, the $\eta_{powertrain}$ is affected by several vehicle parameters, atmosphere and driving conditions. An increase in vehicle M_v leads to the requirement of higher power and torque at the wheel with the same powertrain configurations. This scenario drives the powertrain components to operate in inefficient regions thus lowering the $\eta_{powertrain.}$ Likewise, the aerodynamic parameters such as C_d and A_f have a substantial influence on $\eta_{powertrain}$ as the requirement of P_t at the wheel is high at higher speeds than lower speeds. However, an increase in f_r between tire and road surface with inappropriate tire and road parameters lowers the $\eta_{powertrain}$ at low speeds. Also, it drives the battery to deliver high current for operating the motor at peak torque region, which normally causes higher power losses and results in lower efficiency [226].

The types and sizes of powertrain components along with their configuration predominantly affect the $\eta_{\_powertrain}$. A lower C-rate and inappropriate capacity battery cause higher power losses during the requirement of high power and torque at the wheel. Similarly, motor types and their operating regions play a vital role in variations in $\eta_{\_powertrain}$. Whereas the change in the efficiency of other powertrain components is too low for the entire DC period during simulation [227]. Furthermore, the in-wheel drive EV has more $\eta_{powertrain}$ than EM with different transmission configurations. Eventually, the addition of the final drive in the powertrain causes additional transmission losses and results in a reduction of $\eta_{powertrain}$ [223]. Due to low atmospheric temperatures with higher humidity, the $P_{aux.sys}$ is higher, especially during acceleration at higher grades. As the battery efficiency is highly correlated with its operating temperature, a higher amount of power is utilized to heat the battery and motor to improve its operating characteristics which causes some additional power losses and lowers the $\eta_{powertrain}$ [228]. Also, the frequent acceleration and deceleration significantly affect the $\eta_{powertrain}$ in urban driving conditions owing to the highly frequent switching of motor operating regions and the increase in switching and power losses of the power converter and battery [229].

D. VEHICLE TORQUE AND POWER

The requirement of vehicle torque and power relies on the vehicle parameters, atmosphere and driving conditions. Tractive torque and power requirement at the wheel are increased to maintain the same speed and acceleration time with an increase in M_v as the F_t is increased. Especially, higher T_t is required at low speeds and maintaining higher P_t in the wheel at higher speeds is essential to meet the vehicle's performance. Further, the increase in C_d and A_f causes higher P_t at higher speeds than lower speeds. However, the increase in f_r of tire and wheel slip is more significant at low speeds and requires more T_t to maintain the same acceleration performances [230]. Further, an increase in $P_{aux.sys}$ in cold weather diminishes the capability of powertrain components thus reducing the vehicle's maximum power and torque. The maximum torque and power of an EV also depend on the size and configuration of powertrain components. In the case of the battery, the maximum vehicle torque and power are increased with the use of a higher-capacity battery as it supplies more energy and power to the drivetrain components. Also, the increase in the size of the motor causes higher torque and power at the wheel though the power losses are higher. Additionally, the in-wheel motor drive produces higher power and torque in the wheel due to the absence of a transmission system [231]. Further, the multi-speed transmission increases the maximum wheel torque due to the wide operating ranges of powertrain components but the maximum wheel power is reduced as has lower efficiency than single-speed transmission [223]. The driving conditions and road topography play a critical role in the requirement of wheel torque and power in real-time driving. Whereas the requirement of wheel torque is higher at low speeds on urban DCs and higher wheel power is required at high speeds at highway DCs during simulations. Also, the road surface with a larger grade angle requires higher wheel torque due to higher acceleration [183].

IX. PERFORMANCE ENHANCEMENT TECHNIQUES FOR EV OUTPUT CHARACTERISTICS

Commonly, the EV performance characteristics are improved by increasing the $\eta_{powertrain}$ with lowering torque and power requirements at the wheel during different driving conditions. This can be accomplished by adopting a suitable power source, design and configuration of drivetrain components, thermal management system and lightweight materials [232] as shown in Fig. 17. The use of lightweight, good thermal characteristics, higher current capability and energy density batteries such as lithium-sulphur and lithium-air batteries have improved the DR than li-ion batteries with conventional materials [233]. Also, the use of high-power density and current capability power sources such as super-capacitor and fuel cells with an appropriate energy management strategy improves the DR, acceleration and gradeability by minimizing the EC and M_v. This can be justified by higher

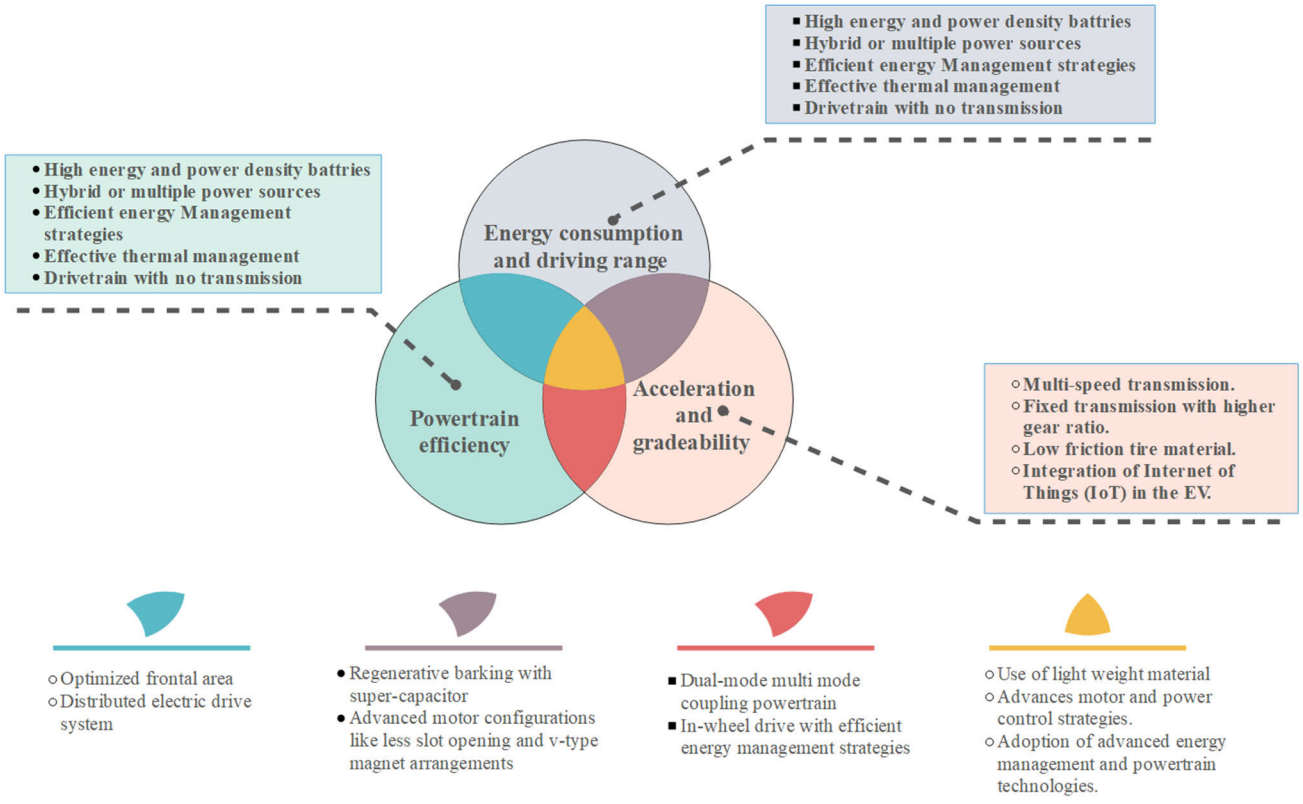

FIGURE 17. Improvisation methods for EV performance characteristics.

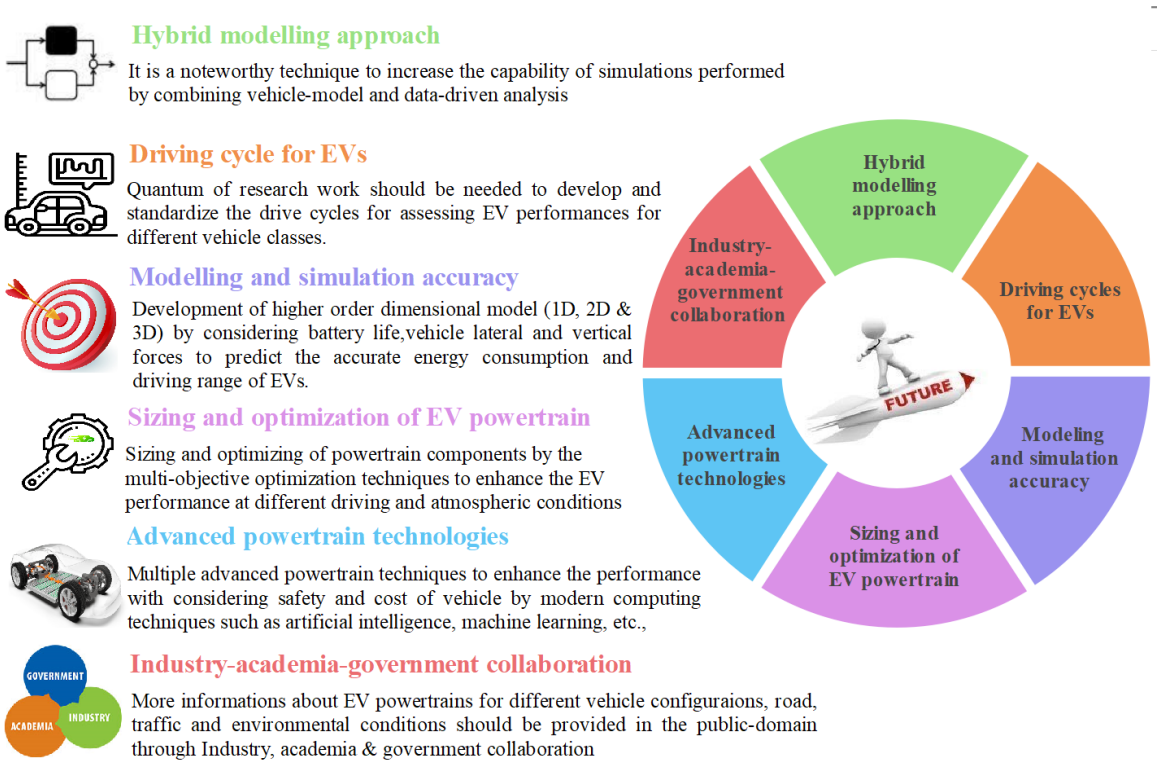

FIGURE 18. Future research direction in modelling and simulation of EV powertrain development.

current capability, powertrain and charging efficiency of super-capacitor and fuel cells [234], [235]. Further, the use of control strategies like PWM, pulse amplitude modulation (PAM) and bang-bang type current control with a super-capacitor and fuel cell improves the DR of EV by minimising the power converter losses [236], [237].

The smaller variation in drivetrain configuration has a greater impact on the performance of EVs than the varying size of drivetrain components. Further, lightweight distributed electric drive systems with adequate torque distribution strategies are improving the DR of EVs more than single-motor drive systems [238]. Also, dual motor with multi-mode coupling powertrain (DMMCP) delivers better DR than other drivetrain configurations. The $\eta_{\text{powertrain}}$ and dynamic performance factors like gradeability, acceleration time and maximum speed are improved with the DMMCP and different energy management strategies as it drives the motor at higher efficiency region during different operating conditions [239]. Besides, motor configurations such as a v-type arrangement of permanent magnet and a lesser slot opening with different modulation techniques such as PWM, PAM, etc. have provided better DR and dynamic performance with lower power losses [240], [241].

The use of regenerative braking with an ultra-capacitor in the EV powertrain increases the regenerative efficiency and DR of EVs [242]. Additionally, Weight reduction of EVs has a greater potential to improve all the aspects of EV performance such as DR, acceleration and gradeability by reducing the EC, torque and power requirement in the wheel [243]. In recent days, M_v has been reduced by replacing conventional materials and powertrain components with advanced materials and powertrain technologies. Also, it is expected to reduce the vehicle weight further to extend the DR and improve the driveability in future [244], [245]. Especially, the use of low-friction tyres and effective thermal management at low-temperature operating conditions improve the ability to accelerate and climb uphill with minimal EC and result in higher DR [246], [247].

X. SUMMARY AND FUTURE SCOPE

This review designates to elaborate the summary of research works in the field on the estimation of EV performance characteristics such as EC, DR, acceleration, gradeability, etc. by analytical method. A cohesive approach is followed in this review to explore the different modelling methods which consist of sub-models with required input data. Further, this study enumerates the characterization of localized DCs and simulation tools used for evaluating EV performance through simulation. Also, a brief discussion has been done on variations in EV performance entities with different input parameters along with its improvisation methods. As a result of the holistic review approach in this research domain, a few major conclusions are highlighted along with possibilities of future research direction as follows.

1) Among these modelling approaches, the analytical model is uncomplicated to understand. However, the accuracy of EC and DR estimation of EVs through an analytical modelling approach is not matched with real-time data.
2) To optimize the EV powertrain design and develop the charging infrastructure in region-specific, the localised DCs are developed for different vehicle classes by many researchers and simulation results of localized DCs have matched with the real-time EC of EVs.
3) In most of the studies, the zero-dimensional EV performance model is developed with longitudinal forces and simulation is commonly executed in MATLAB and Simulink platforms. Further, the performance model for different vehicle classes comprises sub-models with different input conditions and data of EV powertrain components, driving and atmospheric conditions. The accuracy of EV range prediction by the analytical model is solely based on the input data of the above-mentioned sub-models.
4) The influence of different internal and external parameters on EV performance features is analysed with the results of simulation studies for different vehicle configurations, DCs and ambient conditions. In addition, the powertrain simulation studies with different advanced technologies such as hybrid power source, distributed electric drive systems, multi-speed transmission, use of lightweight material and efficient energy management exhibit better performance than the simple electric powertrain.

However, numerous simulation studies are performed to evaluate the EC and DR of EVs. Still, the accuracy of the above-mentioned performance factors through simulation is not matched with real-time data due to the limited information available about powertrain configurations, road and atmospheric conditions. Also, the performance of EVs depends on numerous factors such as driver behaviour, vehicle, atmosphere and road parameters. To eliminate the driver's anxiety about DR and extend the capability of the powertrain, more research works should be focused on developing an efficient electric powertrain with different advanced technologies as shown in Fig. 18. Also, to improve the reliability and prediction accuracy of EV performance features through modelling, the uncertainty on modelling of input data related to vehicle, powertrain components, and atmospheric and road conditions are cautiously considered in future research work. Further, it is necessary to identify the most significant uncertainty parameters with respect to the different EV operating conditions to match the real-time performance values [248], [249]. Thereby, the authors recommend that the aforementioned future research investigations can promote the penetration of EVs in the transportation sector by extending the overall performance.

REFERENCES

[1] I Energy Agency. (2022). *Global EV Outlook 2022 Securing Supplies for an Electric Future*. Accessed: Jan. 13, 2023. [Online]. Available: https://www.iea.org/t&c/

[2] C. Fiori, K. Ahn, and H. A. Rakha, "Microscopic series plug-in hybrid electric vehicle energy consumption model: Model development and validation," *Transp. Res. D, Transp. Environ.*, vol. 63, pp. 175–185, Aug. 2018, doi: 10.1016/j.trd.2018.04.022.

[3] M. Fanesi and D. Scaradozzi, "Optimize the mild hybrid electric vehicles control system to reduce the emission," in *Proc. IEEE 23rd Int. Symp. Consum. Technol. (ISCT)*, Jun. 2019, pp. 317–321, doi: 10.1109/ISCE.2019.8901027.

[4] J. A. Sanguesa, V. Torres-Sanz, P. Garrido, F. J. Martinez, and J. M. Marquez-Barja, "A review on electric vehicles: Technologies and challenges," *Smart Cities*, vol. 4, no. 1, pp. 372–404, Mar. 2021, doi: 10.3390/smartcities4010022.

[5] A. Albatayneh, M. N. Assaf, D. Alterman, and M. Jaradat, "Comparison of the overall energy efficiency for internal combustion engine vehicles and electric vehicles," *Environ. Climate Technol.*, vol. 24, no. 1, pp. 669–680, Jan. 2020, doi: 10.2478/rtuect-2020-0041.

[6] H. Singh, M. Kavianipour, M. Ghamami, and A. Zockaie, "Adoption of autonomous and electric vehicles in private and shared mobility systems," *Transp. Res. D, Transp. Environ.*, vol. 115, Feb. 2023, Art. no. 103561, doi: 10.1016/j.trd.2022.103561.

[7] V. H. Fan, S. Wang, K. Meng, and Z. Y. Dong, "Optimal shared mobility planning for electric vehicles in the distribution network," *IET Gener., Transmiss. Distribution*, vol. 13, no. 11, pp. 2257–2267, Jun. 2019, doi: 10.1049/iet-gtd.2018.6900.

[8] A. Saxena, S. P. Nikam, and B. G. Fernandes, "Study and design of an efficient dual-motor powertrain for two-wheeled electric vehicles," in *Proc. 45th Annu. Conf. IEEE Ind. Electron. Soc.*, vol. 1, Oct. 2019, pp. 2738–2743, doi: 10.1109/IECON.2019.8927120.

[9] H. Vidhya and S. Allirani, "A literature review on electric vehicles: Architecture, electrical machines for power train, converter topologies and control techniques," in *Proc. Int. Conf. Comput. Perform. Eval. (ComPE)*, Dec. 2021, pp. 565–575, doi: 10.1109/ComPE53109.2021.9751896.

[10] L. C. A. Silva, J. J. Eckert, M. A. M. Lourenço, F. L. Silva, F. C. Corrêa, and F. G. Dedini, "Electric vehicle battery-ultracapacitor hybrid energy storage system and drivetrain optimization for a real-world urban driving scenario," *J. Brazilian Soc. Mech. Sci. Eng.*, vol. 43, no. 5, pp. 1–15, May 2021, doi: 10.1007/S40430-021-02975-W.

[11] F. Lei, Y. Bai, W. Zhu, and J. Liu, "A novel approach for electric powertrain optimization considering vehicle power performance, energy consumption and ride comfort," *Energy*, vol. 167, pp. 1040–1050, Jan. 2019, doi: 10.1016/j.energy.2018.11.052.

[12] J. J. Eckert, L. C. de Alkmin Silva, F. G. Dedini, and F. C. Corrêa, "Electric vehicle powertrain and fuzzy control multi-objective optimization, considering dual hybrid energy storage systems," *IEEE Trans. Veh. Technol.*, vol. 69, no. 4, pp. 3773–3782, Apr. 2020, doi: 10.1109/TVT.2020.2973601.

[13] P. Saiteja, B. Ashok, A. S. Wagh, and M. E. Farrag, "Critical review on optimal regenerative braking control system architecture, calibration parameters and development challenges for EVs," *Int. J. Energy Res.*, vol. 46, no. 14, pp. 20146–20179, Nov. 2022, doi: 10.1002/er.8306.

[14] C. Kannan, R. Vignesh, C. Karthick, and B. Ashok, "Critical review towards thermal management systems of lithium-ion batteries in electric vehicle with its electronic control unit and assessment tools," *Proc. Inst. Mech. Eng., D, J. Automobile Eng.*, vol. 235, no. 7, pp. 1783–1807, Jan. 2021, doi: 10.1177/0954407020982865.

[15] B. Ashok, C. Kannan, B. Mason, S. D. Ashok, V. Indragandhi, D. Patel, A. S. Wagh, A. Jain, and C. Kavitha, "Towards safer and smarter design for lithium-ion-battery-powered electric vehicles: A comprehensive review on control strategy architecture of battery management system," *Energies*, vol. 15, no. 12, p. 4227, Jun. 2022, doi: 10.3390/en15124227.

[16] S. Aggarwal and A. K. Singh, "Electric vehicles the future of transportation sector: A review," *Energy Sources, A, Recovery, Utilization, Environ. Effects*, pp. 1–21, Sep. 2021, doi: 10.1080/15567036.2021.1976322.

[17] M. S. Hossain, L. Kumar, M. El Haj Assad, and R. Alayi, "Advancements and future prospects of electric vehicle technologies: A comprehensive review," *Complexity*, vol. 2022, pp. 1–21, Jul. 2022, doi: 10.1155/2022/3304796.

[18] J. Wang, C. Zhang, D. Guo, F. Yang, Z. Zhang, and M. Zhao, "Drive-cycle based configuration design and energy efficiency analysis of dual-motor 4WD system with two-speed transmission for electric vehicles," *IEEE Trans. Transport. Electrific.*, early access, May 18, 2023, doi: 10.1109/TTE.2023.3277479.

[19] C. Kannan, B. Ashok, R. Thirumalaivasan, L. N. S. Reddy, R. S. Rangan, and S. Eashwar, "Evaluation of transmission types and control strategies for electric vehicles," in *Proc. 3rd IEEE Int. Virtual Conf. Innov. Power Adv. Comput. Technol. (i-PACT)*, Nov. 2021, pp. 1–8, doi: 10.1109/I-PACT52855.2021.9697062.

[20] X. Zhu, H. Zhang, J. Xi, J. Wang, and Z. Fang, "Robust speed synchronization control for clutchless automated manual transmission systems in electric vehicles," *Proc. Inst. Mech. Eng., D, J. Automobile Eng.*, vol. 229, no. 4, pp. 424–436, Aug. 2014, doi: 10.1177/0954407014546431.

[21] L. Kumar, K. K. Gupta, and S. Jain, "Architecture and configuration of electrified vehicles: A review," in *Proc. IEEE Int. Symp. Ind. Electron.*, May 2013, pp. 1–6, doi: 10.1109/ISIE.2013.6563825.

[22] P. Fafoutellis, E. G. Mantouka, and E. I. Vlahogianni, "Eco-driving and its impacts on fuel efficiency: An overview of technologies and data-driven methods," *Sustainability*, vol. 13, no. 1, p. 226, Dec. 2020, doi: 10.3390/su13010226.

[23] Y.-W. Chung, B. Khaki, T. Li, C. Chu, and R. Gadh, "Ensemble machine learning-based algorithm for electric vehicle user behavior prediction," *Appl. Energy*, vol. 254, Nov. 2019, Art. no. 113732, doi: 10.1016/j.apenergy.2019.113732.

[24] B. Luin, S. Petelin, and F. Al-Mansour, "Microsimulation of electric vehicle energy consumption," *Energy*, vol. 174, pp. 24–32, May 2019, doi: 10.1016/j.energy.2019.02.034.

[25] Y. Al-Wreikat, C. Serrano, and J. R. Sodré, "Driving behaviour and trip condition effects on the energy consumption of an electric vehicle under real-world driving," *Appl. Energy*, vol. 297, Sep. 2021, Art. no. 117096, doi: 10.1016/j.apenergy.2021.117096.

[26] F. L. Mapelli, D. Tarsitano, F. L. Mapelli, and D. Tarsitano, "Modeling of full electric and hybrid electric vehicles," in *New Generation of Electric Vehicles*, Dec. 2012, doi: 10.5772/53570.

[27] X. Qi, G. Wu, K. Boriboonsomsin, and M. J. Barth, "Data-driven decomposition analysis and estimation of link-level electric vehicle energy consumption under real-world traffic conditions," *Transp. Res. Part D: Transp. Environ.*, vol. 64, pp. 36–52, Oct. 2018, doi: 10.1016/j.trd.2017.08.008.

[28] H. Xiong, H. Liu, R. Zhang, L. Yu, Z. Zong, M. Zhang, and Z. Li, "An energy matching method for battery electric vehicle and hydrogen fuel cell vehicle based on source energy consumption rate," *Int. J. Hydrogen Energy*, vol. 44, no. 56, pp. 29733–29742, Nov. 2019, doi: 10.1016/j.ijhydene.2019.02.169.

[29] Z. Yi and P. H. Bauer, "Adaptive multiresolution energy consumption prediction for electric vehicles," *IEEE Trans. Veh. Technol.*, vol. 66, no. 11, pp. 10515–10525, Nov. 2017, doi: 10.1109/TVT.2017.2720587.

[30] X. Lin, Y. Li, and G. Zhang, "Bi-objective optimization strategy of energy consumption and shift shock based driving cycle-aware bias coefficients for a novel dual-motor electric vehicle," *Energy*, vol. 249, Jun. 2022, Art. no. 123596, doi: 10.1016/j.energy.2022.123596.

[31] R. Zhang and E. Yao, "Electric vehicles' energy consumption estimation with real driving condition data," *Transp. Res. D, Transp. Environ.*, vol. 41, pp. 177–187, Dec. 2015, doi: 10.1016/j.trd.2015.10.010.

[32] X. Wu, D. Freese, A. Cabrera, and W. A. Kitch, "Electric vehicles' energy consumption measurement and estimation," *Transp. Res. D, Transp. Environ.*, vol. 34, pp. 52–67, Jan. 2015, doi: 10.1016/j.trd.2014.10.007.

[33] C. Fiori, K. Ahn, and H. A. Rakha, "Power-based electric vehicle energy consumption model: Model development and validation," *Appl. Energy*, vol. 168, pp. 257–268, Apr. 2016, doi: 10.1016/j.apenergy.2016.01.097.

[34] C. De Cauwer, J. Van Mierlo, and T. Coosemans, "Energy consumption prediction for electric vehicles based on real-world data," *Energies*, vol. 8, no. 8, pp. 8573–8593, Aug. 2015, doi: 10.3390/en8088573.

[35] C. De Cauwer, W. Verbeke, T. Coosemans, S. Faid, and J. Van Mierlo, "A data-driven method for energy consumption prediction and energy-efficient routing of electric vehicles in real-world conditions," *Energies*, vol. 10, no. 5, p. 608, May 2017, doi: 10.3390/en10050608.

[36] J. Hong, S. Park, and N. Chang, "Accurate remaining range estimation for electric vehicles," in *Proc. 21st Asia South Pacific Design Autom. Conf. (ASP-DAC)*, Jan. 2016, pp. 781–786, doi: 10.1109/ASP-DAC.2016.7428106.

[37] W. Li, P. Stanula, P. Egede, S. Kara, and C. Herrmann, "Determining the main factors influencing the energy consumption of electric vehicles in the usage phase," *Proc. CIRP*, vol. 48, pp. 352–357, Jan. 2016, doi: 10.1016/j.procir.2016.03.014.

[38] F. Morlock, B. Rolle, M. Bauer, and O. Sawodny, "Forecasts of electric vehicle energy consumption based on characteristic speed profiles and real-time traffic data," *IEEE Trans. Veh. Technol.*, vol. 69, no. 2, pp. 1404–1418, Feb. 2020, doi: 10.1109/TVT.2019.2957536.

[39] H. Wang, D. Zhao, Y. Cai, Q. Meng, and G. P. Ong, "A trajectory-based energy consumption estimation method considering battery degradation for an urban electric vehicle network," *Transp. Res. Part D: Transp. Environ.*, vol. 74, pp. 142–153, Sep. 2019, doi: 10.1016/j.trd.2019.07.021.

[40] H. Wang, D. Zhao, Q. Meng, G. P. Ong, and D.-H. Lee, "Network-level energy consumption estimation for electric vehicles considering vehicle and user heterogeneity," *Transp. Res. A, Policy Pract.*, vol. 132, pp. 30–46, Feb. 2020, doi: 10.1016/j.tra.2019.10.010.

[41] J. Yao and A. Moawad, "Vehicle energy consumption estimation using large scale simulations and machine learning methods," *Transp. Res. C, Emerg. Technol.*, vol. 101, pp. 276–296, Apr. 2019, doi: 10.1016/j.trc.2019.02.012.

[42] L. Zhao, W. Yao, Y. Wang, and J. Hu, "Machine learning-based method for remaining range prediction of electric vehicles," *IEEE Access*, vol. 8, pp. 212423–212441, 2020, doi: 10.1109/ACCESS.2020.3039815.

[43] W. Tu, P. Santi, T. Zhao, X. He, Q. Li, L. Dong, T. J. Wallington, and C. Ratti, "Acceptability, energy consumption, and costs of electric vehicle for ride-hailing drivers in Beijing," *Appl. Energy*, vol. 250, pp. 147–160, Sep. 2019, doi: 10.1016/j.apenergy.2019.04.157.

[44] S. K. Vempalli, J. Ramprabhakar, S. Shankar, and G. Prabhakar, "Electric vehicle designing, modelling and simulation," in *Proc. 4th Int. Conf. Converg. Technol. (I2CT)*, Oct. 2018, pp. 1–6, doi: 10.1109/I2CT42659.2018.9058161.

[45] D. Qin, J. Li, T. Wang, and D. Zhang, "Modeling and simulating a battery for an electric vehicle based on modelica," *Automot. Innov.*, vol. 2, no. 3, pp. 169–177, Sep. 2019, doi: 10.1007/S42154-019-00066-0.

[46] M. Yaich, M. R. Hachicha, and M. Ghariani, "Modeling and simulation of electric and hybrid vehicles for recreational vehicle," in *Proc. 16th Int. Conf. Sci. Techn. Autom. Control Comput. Eng. (STA)*, Dec. 2015, pp. 181–187, doi: 10.1109/STA.2015.7505098.

[47] K. Mahmud and G. E. Town, "A review of computer tools for analyzing the impact of electric vehicles on power distribution," in *Proc. Australas. Universities Power Eng. Conf. (AUPEC)*, Sep. 2015, pp. 1–6, doi: 10.1109/AUPEC.2015.7324853.

[48] P. Saiteja, B. Ashok, B. Mason, and S. Krishna, "Development of efficient energy management strategy to mitigate speed and torque ripples in SR motor through adaptive supervisory self-learning technique for electric vehicles," *IEEE Access*, vol. 11, pp. 96460–96484, 2023, doi: 10.1109/ACCESS.2023.3311851.

[49] X. Xu, H. M. A. Aziz, and R. Guensler, "A modal-based approach for estimating electric vehicle energy consumption in transportation networks," *Transp. Res. D, Transp. Environ.*, vol. 75, pp. 249–264, Oct. 2019, doi: 10.1016/j.trd.2019.09.001.

[50] M. S. B. Ahmad, A. Pesyridis, P. Sphicas, A. M. Andwari, A. Gharehghani, and B. M. Vaglieco, "Electric vehicle modelling for future technology and market penetration analysis," *Frontiers Mech. Eng.*, vol. 8, p. 61, Jul. 2022, doi: 10.3389/FMECH.2022.896547.

[51] M. Etxandi-Santolaya, L. Canals Casals, and C. Corchero, "Estimation of electric vehicle battery capacity requirements based on synthetic cycles," *Transp. Res. D, Transp. Environ.*, vol. 114, Jan. 2023, Art. no. 103545, doi: 10.1016/j.trd.2022.103545.

[52] A. Fotouhi, D. J. Auger, K. Propp, S. Longo, and M. Wild, "A review on electric vehicle battery modelling: From lithium-ion toward lithium–sulphur," *Renew. Sustain. Energy Rev.*, vol. 56, pp. 1008–1021, Apr. 2016, doi: 10.1016/j.rser.2015.12.009.

[53] Y. Chen, G. Wu, R. Sun, A. Dubey, A. Laszka, and P. Pugliese, "A review and outlook on energy consumption estimation models for electric vehicles," *SAE Int. J. Sustain. Transp., Energy, Environ., Policy*, vol. 2, no. 1, p. 5, Mar. 2021, doi: 10.4271/13-02-01-0005.

[54] Q. Wang, B. Jiang, B. Li, and Y. Yan, "A critical review of thermal management models and solutions of lithium-ion batteries for the development of pure electric vehicles," *Renew. Sustain. Energy Rev.*, vol. 64, pp. 106–128, Oct. 2016, doi: 10.1016/j.rser.2016.05.033.

[55] C. Ye, W. He, and H. Chen, "Electric vehicle routing models and solution algorithms in logistics distribution: A systematic review," *Environ. Sci. Pollut. Res.*, vol. 29, no. 38, pp. 57067–57090, Aug. 2022, doi: 10.1007/S11356-022-21559-2.

[56] M. Shepero, J. Munkhammar, J. Widén, J. D. K. Bishop, and T. Boström, "Modeling of photovoltaic power generation and electric vehicles charging on city-scale: A review," *Renew. Sustain. Energy Rev.*, vol. 89, pp. 61–71, Jun. 2018, doi: 10.1016/j.rser.2018.02.034.

[57] Y. Amara-Ouali, Y. Goude, P. Massart, J.-M. Poggi, and H. Yan, "A review of electric vehicle load open data and models," *Energies*, vol. 14, no. 8, p. 2233, Apr. 2021, doi: 10.3390/en14082233.

[58] A. Di Martino, S. M. Miraftabzadeh, and M. Longo, "Strategies for the modelisation of electric vehicle energy consumption: A review," *Energies*, vol. 15, no. 21, p. 8115, Oct. 2022, doi: 10.3390/en15218115.

[59] G. Saldaña, J. I. San Martín, I. Zamora, F. J. Asensio, and O. Oñederra, "Analysis of the current electric battery models for electric vehicle simulation," *Energies*, vol. 12, no. 14, p. 2750, Jul. 2019, doi: 10.3390/en12142750.

[60] Y. Xiao, Y. Zhang, I. Kaku, R. Kang, and X. Pan, "Electric vehicle routing problem: A systematic review and a new comprehensive model with nonlinear energy recharging and consumption," *Renew. Sustain. Energy Rev.*, vol. 151, Nov. 2021, Art. no. 111567, doi: 10.1016/j.rser.2021.111567.

[61] E. A. Lomonova, J. J. H. Paulides, S. Wilkins, and J. Tegenbosch, "ADEPT: 'ADvanced electric powertrain technology'—Virtual and hardware platforms," in *Proc. 10th Int. Conf. Ecological Vehicles Renew. Energies (EVER)*, Mar. 2015, pp. 1–10, doi: 10.1109/EVER.2015.7112976.

[62] P. Othaganont, F. Assadian, and D. J. Auger, "Multi-objective optimisation for battery electric vehicle powertrain topologies," *Proc. Inst. Mech. Eng., D, J. Automobile Eng.*, vol. 231, no. 8, pp. 1046–1065, Jul. 2017, doi: 10.1177/0954407016671275.

[63] G. Mohan, F. Assadian, and S. Longo, "Comparative analysis of forward-facing models vs backwardfacing models in powertrain component sizing," in *Proc. IET Hybrid Electric Vehicles Conf. (HEVC)*, Nov. 2013, pp. 1–6, doi: 10.1049/cp.2013.1920.

[64] P. Pettersson, B. Jacobson, F. Bruzelius, P. Johannesson, and L. Fast, "Intrinsic differences between backward and forward vehicle simulation models," *IFAC-PapersOnLine*, vol. 53, no. 2, pp. 14292–14299, Jan. 2020, doi: 10.1016/j.ifacol.2020.12.1368.

[65] A. A. Abulifa, A. C. Soh, M. K. Hassan, R. M. K. R. Ahamd, and M. A. Mohdradzi, "Mathematical modelling and simulation of battery electric vehicle based on backward-facing approach technique," *Turkish J. Comput. Math. Educ.*, vol. 12, no. 14, pp. 1–10, 2021.

[66] G. R. Mineeshma, R. V. Chacko, S. Amal, M. L. Sreedevi, and V. Vishnu, "Component sizing of electric vehicle / hybrid electric vehicle subsystems using backward modelling approach," in *Proc. IEEE Int. Conf. Power Electron., Drives Energy Syst. (PEDES)*, Dec. 2016, pp. 1–5, doi: 10.1109/PEDES.2016.7914227.

[67] K. Atamnia, A. Lebaroud, and S. Adikari, "Forward-looking model dedicated to the study of electric vehicle range considering drive cycles," *Sci. Bull. Electr. Eng. Fac.*, vol. 21, no. 1, pp. 52–59, Apr. 2021, doi: 10.2478/sbeef-2021-0011.

[68] L. Zhang, L. Li, B. Qi, and J. Song, "Configuration analysis and performance comparison of drive systems for pure electric vehicle," SAE, Warrendale, PA, USA, Tech. Papers 2015-01-1165, Apr. 2015, doi: 10.4271/2015-01-1165.

[69] G. Dixon, R. Stobart, and T. Steffen, "Unified backwards facing and forwards facing simulation of a hybrid electric vehicle using MATLAB Simscape," SAE, Warrendale, PA, USA, Tech. Papers 2015-01-1215, Apr. 2015, doi: 10.4271/2015-01-1215.

[70] K. H. Hauer and R. M. Moore, "Fuel cell vehicle simulation—Part 1: Benchmarking available fuel cell vehicle simulation tools," *Fuel Cells*, vol. 3, no. 3, pp. 84–94, Nov. 2003, doi: 10.1002/fuce.200332102.

[71] M. Serda, "Simulation methodologies for innovative vehicle drive systems," *Uniwersytet Sląski*, vol. 7, no. 1, pp. 343–354, Sep. 2004, doi: 10.2/JQUERY.MIN.JS.

[72] A. Desreveaux, A. Bouscayrol, R. Trigui, E. Hittinger, E. Castex, and G. M. Sirbu, "Accurate energy consumption for comparison of climate change impact of thermal and electric vehicles," *Energy*, vol. 268, Apr. 2023, Art. no. 126637, doi: 10.1016/j.energy.2023.126637.

[73] C. Duangtongsuk, T. Thianthamthita, R. Pupadubsin, N. Chayopitak, and W. Kongprawechnon, "EV conversion performance analysis and sizing of traction motor and battery from driving cycles," in *Proc. 19th Int. Conf. Electr. Eng./Electron., Comput., Telecommun. Inf. Technol. (ECTI-CON)*, May 2022, pp. 1–6, doi: 10.1109/ECTI-CON54298.2022.9795372.

[74] M. Pfriem and F. Gauterin, "Development of real-world driving cycles for battery electric vehicles," *World Electric Vehicle J.*, vol. 8, no. 1, pp. 14–24, Mar. 2016, doi: 10.3390/wevj8010014.

[75] A. K. Singh, A. Dalal, and P. Kumar, "Analysis of induction motor for electric vehicle application based on drive cycle analysis," in *Proc. IEEE Int. Conf. Power Electron., Drives Energy Syst. (PEDES)*, Dec. 2014, pp. 1–6, doi: 10.1109/PEDES.2014.7042134.

[76] V. Parekh and V. Shah, "Measurement and analysis of Indian road drive cycles for efficient and economic design of HEV component," *World Electric Vehicle J.*, vol. 7, no. 1, pp. 121–132, Mar. 2015, doi: 10.3390/wevj7010121.

[77] H. Y. Tong, "Development of a driving cycle for a supercapacitor electric bus route in Hong Kong," *Sustain. Cities Soc.*, vol. 48, Jul. 2019, Art. no. 101588, doi: 10.1016/j.scs.2019.101588.

[78] F. Guo and F. Zhang, "A study of driving cycle for electric cars on Beijing urban and suburban roads," in *Proc. IEEE Int. Conf. Power Renew. Energy (ICPRE)*, Oct. 2016, pp. 319–322, doi: 10.1109/ICPRE.2016.7871224.

[79] C. Chandrashekar, P. Agrawal, P. Chatterjee, and D. S. Pawar, "Development of E-rickshaw driving cycle (ERDC) based on micro-trip segments using random selection and K-means clustering techniques," *IATSS Res.*, vol. 45, no. 4, pp. 551–560, Dec. 2021, doi: 10.1016/j.iatssr.2021.07.001.

[80] F. Chen, S. Zhou, Y. Hua, X. Zhou, X. Liu, N. Wu, J. Xiu, and S. Yang, "A novel method of developing driving cycle for electric vehicles to evaluate the private driving habits," *IEEE Access*, vol. 9, pp. 46476–46486, 2021, doi: 10.1109/ACCESS.2021.3049411.

[81] S. K. Mayakuntla and A. Verma, "A novel methodology for construction of driving cycles for Indian cities," *Transp. Res. Part D: Transp. Environ.*, vol. 65, pp. 725–735, Dec. 2018, doi: 10.1016/j.trd.2018.10.013.

[82] S. K. Rechkemmer, "Towards a Shanghai electric two-wheeler cycle (SE2WC)," in *Proc. 12th Asian Control Conf. (ASCC)*, Jan. 2023, pp. 319–324. [Online]. Available: https://ieeexplore.ieee.org/document/8765091

[83] S. K. Rechkemmer, X. Zang, A. Boronka, W. Zhang, and O. Sawodny, "Utilization of smartphone data for driving cycle synthesis based on electric two-wheelers in Shanghai," *IEEE Trans. Intell. Transp. Syst.*, vol. 22, no. 2, pp. 876–886, Feb. 2021, doi: 10.1109/TITS.2019.2961179.

[84] S. K. Pathak, Y. Singh, V. Sood, and S. A. Channiwala, "Drive cycle development for electrical three wheelers," SAE, Warrendale, PA, USA, Tech. Papers 2017-01-1593, Mar. 2017, doi: 10.4271/2017-01-1593.

[85] X. Zhao, Q. Yu, J. Ma, Y. Wu, M. Yu, and Y. Ye, "Development of a representative EV urban driving cycle based on a K-means and SVM hybrid clustering algorithm," *J. Adv. Transp.*, vol. 2018, pp. 1–18, Nov. 2018, doi: 10.1155/2018/1890753.

[86] J. Brady and M. O'Mahony, "Development of a driving cycle to evaluate the energy economy of electric vehicles in urban areas," *Appl. Energy*, vol. 177, pp. 165–178, Sep. 2016, doi: 10.1016/j.apenergy.2016.05.094.

[87] Z. Jing, G. Wang, S. Zhang, and C. Qiu, "Building Tianjin driving cycle based on linear discriminant analysis," *Transp. Res. D, Transp. Environ.*, vol. 53, pp. 78–87, Jun. 2017, doi: 10.1016/j.trd.2017.04.005.

[88] X. Zhao, Y. Ye, J. Ma, P. Shi, and H. Chen, "Construction of electric vehicle driving cycle for studying electric vehicle energy consumption and equivalent emissions," *Environ. Sci. Pollut. Res.*, vol. 27, no. 30, pp. 37395–37409, Oct. 2020, doi: 10.1007/S11356-020-09094-4.

[89] S. Tewiele, P. Driesch, T. Weber, and D. Schramm, "Clustering of real BEV driving data with subsequent driving cycle construction using Markov chains," in *Proc. Automot. Meets Electron. 9th GMM-Symp.*, Jan. 2023, pp. 1–6. [Online]. Available: https://ieeexplore.ieee.org/document/8402811

[90] U. Previti, A. Galvagno, G. Risitano, and F. Alberti, "Smart design: Application of an automatic new methodology for the energy assessment and redesign of hybrid electric vehicle mechanical components," *Vehicles*, vol. 4, no. 2, pp. 586–607, Jun. 2022, doi: 10.3390/vehicles4020034.

[91] A. Falai, T. A. Giuliacci, D. Misul, G. Paolieri, and P. G. Anselma, "Modeling and on-road testing of an electric two-wheeler towards range prediction and BMS integration," *Energies*, vol. 15, no. 7, p. 2431, Mar. 2022, doi: 10.3390/en15072431.

[92] M. H. R. Miranda, F. L. Silva, M. A. M. Lourenço, J. J. Eckert, and L. C. A. Silva, "Electric vehicle powertrain and fuzzy controller optimization using a planar dynamics simulation based on a real-world driving cycle," *Energy*, vol. 238, Jan. 2022, Art. no. 121979, doi: 10.1016/j.energy.2021.121979.

[93] S. Schnelle, J. Wang, R. Jagacinski, and H.-J. Su, "A feedforward and feedback integrated lateral and longitudinal driver model for personalized advanced driver assistance systems," *Mechatronics*, vol. 50, pp. 177–188, Apr. 2018, doi: 10.1016/j.mechatronics.2018.02.007.

[94] A. A. Abulifa, R. K. R. Ahmad, A. C. Soh, M. A. M. Radzi, and M. K. Hassan, "Modelling and simulation of battery electric vehicle by using MATLAB-simulink," in *Proc. IEEE 15th student Conf. Res. Develop. (SCOReD)*, Dec. 2017, pp. 383–387, doi: 10.1109/SCORED.2017.8305360.

[95] Z. Gao, T. LaClair, S. Ou, S. Huff, G. Wu, P. Hao, K. Boriboonsomsin, and M. Barth, "Evaluation of electric vehicle component performance over eco-driving cycles," *Energy*, vol. 172, pp. 823–839, Apr. 2019, doi: 10.1016/j.energy.2019.02.017.

[96] V. Tomar, A. Chitra, D. Krishnachaitanya, N. S. R. Rao, and W. Raziasultana, "Design of powertrain model for an electric vehicle using MATLAB/Simulink," in *Proc. Innov. Power Adv. Comput. Technol. (i-PACT)*, Nov. 2021, pp. 1–7, doi: 10.1109/i-PACT52855.2021.9696518.

[97] C. Montaleza, P. Arévalo, M. Tostado-Véliz, and F. Jurado, "Intrinsic characteristics of forward simulation modeling electric vehicle for energy analysis," *Electricity*, vol. 3, no. 2, pp. 202–219, May 2022, doi: 10.3390/electricity3020012.

[98] S. Alegre, J. V. Míguez, and J. Carpio, "Modelling of electric and parallel-hybrid electric vehicle using MATLAB/Simulink environment and planning of charging stations through a geographic information system and genetic algorithms," *Renew. Sustain. Energy Rev.*, vol. 74, pp. 1020–1027, Jul. 2017, doi: 10.1016/j.rser.2017.03.041.

[99] P. Deshmukh, "Forward-looking, velocity-driven, powertrain modeling and optimal control for continuous variable transmission," Master Sci. Eng., Dept. Mech. Aerosp. Eng., Western Michigan Univ., Kalamazoo, MI, USA, 2018. [Online]. Available: https://scholarworks.wmich.edu/masters_theses

[100] H. Zhao, W. Chen, J. Zhao, Y. Zhang, and H. Chen, "Modular integrated longitudinal, lateral, and vertical vehicle stability control for distributed electric vehicles," *IEEE Trans. Veh. Technol.*, vol. 68, no. 2, pp. 1327–1338, Feb. 2019, doi: 10.1109/TVT.2018.2890228.

[101] G. Ning, L. Xiong, L. Zhang, and Z. Yu, "Method of electric powertrain matching for battery-powered electric cars," *Chin. J. Mech. Eng.*, vol. 26, no. 3, pp. 483–491, May 2013, doi: 10.3901/cjme.2013.03.483.

[102] B. Sri Kaloko, M. Soebagio, and M. Hery Purnomo, "Design and development of small electric vehicle using MATLAB/Simulink," *Int. J. Comput. Appl.*, vol. 24, no. 6, pp. 19–23, Jun. 2011.

[103] N. Ba Hung, S. Jaewon, and O. Lim, "A study of the effects of input parameters on the dynamics and required power of an electric bicycle," *Appl. Energy*, vol. 204, pp. 1347–1362, Oct. 2017, doi: 10.1016/j.apenergy.2017.03.025.

[104] Y. Xu, Y. Zheng, and Y. Yang, "On the movement simulations of electric vehicles: A behavioral model-based approach," *Appl. Energy*, vol. 283, Feb. 2021, Art. no. 116356, doi: 10.1016/j.apenergy.2020.116356.

[105] F. Adegbohun, A. von Jouanne, B. Phillips, E. Agamloh, and A. Yokochi, "High performance electric vehicle powertrain modeling, simulation and validation," *Energies*, vol. 14, no. 5, p. 1493, Mar. 2021, doi: 10.3390/en14051493.

[106] S. Saxena, A. Gopal, and A. Phadke, "Electrical consumption of two-, three- and four-wheel light-duty electric vehicles in India," *Appl. Energy*, vol. 115, pp. 582–590, Feb. 2014, doi: 10.1016/j.apenergy.2013.10.043.

[107] Y. Inoue, T. Kosaka, H. Matsumori, and N. Matsui, "Modeling and simulation of battery-powered electric vehicle on MATLAB/Simulink," in *Proc. 24th Int. Conf. Electr. Mach. Syst. (ICEMS)*, Oct. 2021, pp. 694–698, doi: 10.23919/ICEMS52562.2021.9634585.

[108] S.-H. Lee, T.-H. Kim, and J.-W. Ahn, "Electric powertrain system for E-scooter with rear two in-wheeled propulsion motors," in *Proc. Int. Conf. Electr. Mach. Syst. (ICEMS)*, Oct. 2013, pp. 1491–1493, doi: 10.1109/ICEMS.2013.6754416.

[109] T. Hofman, S. G. van der Tas, W. Ooms, E. W. P. van Meijl, and B. M. Laugeman, "Development of a micro-hybrid system for a three-wheeled motor taxi," *World Electric Vehicle J.*, vol. 3, no. 3, pp. 572–580, Sep. 2009, doi: 10.3390/wevj3030572.

[110] R. Sanjarbek, J. Mavlonov, and A. Mukhitdinov, "Analysis of the powertrain component size of electrified vehicles commercially available on the market," *Commun. Sci. Lett. Univ. Zilina*, vol. 24, no. 1, pp. B74–B86, Jan. 2022, doi: 10.26552/com.c.2022.1.b74-b86.

[111] K. N. Genikomsakis and G. Mitrentsis, "A computationally efficient simulation model for estimating energy consumption of electric vehicles in the context of route planning applications," *Transp. Res. D, Transp. Environ.*, vol. 50, pp. 98–118, Jan. 2017, doi: 10.1016/j.trd.2016.10.014.

[112] W. Gołębiewski and M. Lisowski, "Theoretical analysis of electric vehicle energy consumption according to different driving cycles," *IOP Conf. Ser., Mater. Sci. Eng.*, vol. 421, Oct. 2018, Art. no. 022010, doi: 10.1088/1757-899X/421/2/022010.

[113] M. N. Yuniarto, S. E. Wiratno, Y. U. Nugraha, I. Sidharta, and A. Nasruddin, "Modeling, simulation, and validation of an electric scooter energy consumption model: A case study of Indonesian electric scooter," *IEEE Access*, vol. 10, pp. 48510–48522, 2022, doi: 10.1109/ACCESS.2022.3171860.

[114] S. Rajendran, S. K. Spurgeon, G. Tsampardoukas, and R. Hampson, "Estimation of road frictional force and wheel slip for effective antilock braking system (ABS) control," *Int. J. Robust Nonlinear Control*, vol. 29, no. 3, pp. 736–765, Feb. 2019, doi: 10.1002/rnc.4366.

[115] J. Wang, I. Besselink, and H. Nijmeijer, "Battery electric vehicle energy consumption modelling for range estimation," *Int. J. Electr. Hybrid Vehicles*, vol. 9, no. 2, p. 79, 2017, doi: 10.1504/ijehv.2017.085336.

[116] L. Soni, S. Venkateswaran, and V. Ramachandran, "Performance and comfort optimization from ABS/CBS/motor regenerative braking in an electric two wheeler during heavy and mild braking respectively," SAE, Warrendale, PA, USA, Tech. Papers 2019-26-0122, Jan. 2019, doi: 10.4271/2019-26-0122.

[117] M. Ehsani, *Modern Electric, Hybrid Electric, and Fuel Cell Vehicles*, 3rd ed. CRC Press, Feb. 2018, doi: 10.1201/9780429504884.

[118] P. Prochazka, I. Pazdera, P. Vorel, and D. Cervinka, "Design of small electric car," in *Proc. Int. Symp. Power Electron. Power Electron., Electr. Drives, Autom. Motion*, Jun. 2012, pp. 359–364, doi: 10.1109/SPEEDAM.2012.6264622.

[119] A. Elmarakbi, A. Morris, Q. Ren, and M. Elkady, "Modelling and analyzing electric vehicles with geared transmission systems: Enhancement of energy consumption and performance," *Int. J. Eng. Res. Technol. (IJERT)*, vol. 2, no. 11, 2013, Art. no. IJERTV2IS110249. [Online]. Available: https://www.ijert.org

[120] P. G. Anselma and G. Belingardi, "Comparing battery electric vehicle powertrains through rapid component sizing," *Int. J. Electric Hybrid Vehicles*, vol. 11, no. 1, p. 36, 2019, doi: 10.1504/ijehv.2019.098718.

[121] N. Hinov, P. Punov, B. Gilev, and G. Vacheva, "Model-based estimation of transmission gear ratio for driving energy consumption of an EV," *Electronics*, vol. 10, no. 13, p. 1530, Jun. 2021, doi: 10.3390/electronics10131530.

[122] S. Wolff, S. Kalt, M. Bstieler, and M. Lienkamp, "Influence of powertrain topology and electric machine design on efficiency of battery electric trucks—A simulative case-study," *Energies*, vol. 14, no. 2, p. 328, Jan. 2021, doi: 10.3390/en14020328.

[123] R. E. Araújo, H. Teixeira, J. Barbosa, and V. Leite, "A low cost induction motor controller for light electric vehicles in local areas," in *Proc. IEEE Int. Symp. Ind. Electron.*, vol. 4, Dec. 2005, pp. 1499–1504, doi: 10.1109/ISIE.2005.1529154.

[124] F. J. R. Verbruggen, E. Silvas, and T. Hofman, "Electric powertrain topology analysis and design for heavy-duty trucks," *Energies*, vol. 13, no. 10, p. 2434, May 2020, doi: 10.3390/en13102434.

[125] N. Hashemnia and B. Asaei, "Comparative study of using different electric motors in the electric vehicles," in *Proc. 18th Int. Conf. Electr. Mach.*, Sep. 2008, doi: 10.1109/icelmach.2008.4800157.

[126] E. A. Grunditz and T. Thiringer, "Electric vehicle acceleration performance and motor drive cycle energy efficiency trade-off," in *Proc. XIII Int. Conf. Electr. Mach. (ICEM)*, Sep. 2018, pp. 717–723, doi: 10.1109/ICELMACH.2018.8507201.

[127] A. Semon and A. Craciunescu, "Study to increase the efficiency of the electric drive system of a vehicle at different speeds," in *Proc. 11th Int. Symp. Adv. Topics Electr. Eng. (ATEE)*, Mar. 2019, pp. 1–7, doi: 10.1109/ATEE.2019.8724976.

[128] A. Mahmoudi, W. L. Soong, G. Pellegrino, and E. Armando, "Efficiency maps of electrical machines," in *Proc. IEEE Energy Convers. Congr. Expo. (ECCE)*, Sep. 2015, pp. 2791–2799, doi: 10.1109/ECCE.2015.7310051.

[129] M. Sundaram, M. Anand, J. Chelladurai, P. Varunraj, S. J. Smith, S. Sharma, M. E. H. Assad, and R. Alayi, "Design and FEM analysis of high-torque power density permanent magnet synchronous motor (PMSM) for two-wheeler e-vehicle applications," *Int. Trans. Electr. Energy Syst.*, vol. 2022, pp. 1–14, Jul. 2022, doi: 10.1155/2022/1217250.

[130] H. Mokhtari and E. Tara, "Efficiency map of a switched reluctance motor using finite element method in vehicular applications," in *Proc. 7th Int. Conf. Power Electron.*, Oct. 2007, pp. 644–649, doi: 10.1109/icpe.2007.4692467.

[131] T. Nag, S. B. Santra, A. Chatterjee, D. Chatterjee, and A. K. Ganguli, "Modelling and minimization of losses for brushless DC (BLDC) motor suitable for electric vehicular applications," *UK World J. Model. Simul.*, vol. 1, no. 4, pp. 259–267, 2016.

[132] J. Larminie and J. Lowry, *Electric Vehicle Technology Explained*. Hoboken, NJ, USA: Wiley, 2012. Accessed: Jan. 17, 2023. [Online]. Available: https://www.wiley.com/en-us/Electric+Vehicle+Technology+Explained%2C+2nd+Edition-p-9781119942733

[133] S. O. Kwon, J. J. Lee, B. H. Lee, J. H. Kim, K. H. Ha, and J. P. Hong, "Loss distribution of three-phase induction motor and BLDC motor according to core materials and operating," *IEEE Trans. Magn.*, vol. 45, no. 10, pp. 4740–4743, Oct. 2009, doi: 10.1109/tmag.2009.2022749.

[134] N. A. Kumar and A. S. Joseph, "Retrofitting of conventional two-wheelers to electric two-wheelers," in *Proc. 13th IEEE PES Asia–Pacific Power Energy Eng. Conf. (APPEEC)*, Nov. 2021, pp. 1–8, doi: 10.1109/APPEEC50844.2021.9687799.

[135] K. Venkatachalam, C. R. Sullivan, T. Abdallah, and H. Tacca, "Accurate prediction of ferrite core loss with nonsinusoidal waveforms using only steinmetz parameters," in *Proc. IEEE Workshop Comput. Power Electron., Proceedings.*, 2002, pp. 36–41, doi: 10.1109/cipe.2002.1196712.

[136] Z.-Q. Zhu, S. Xue, W. Chu, J. Feng, S. Guo, Z. Chen, and J. Peng, "Evaluation of iron loss models in electrical machines," *IEEE Trans. Ind. Appl.*, vol. 55, no. 2, pp. 1461–1472, Mar. 2019, doi: 10.1109/TIA.2018.2880674.

[137] S. P. Emami, E. Roshandel, A. Mahmoudi, and S. Khaourzade, "IPM motor optimization for electric vehicles considering driving cycles," in *Proc. 31st Australas. Universities Power Eng. Conf. (AUPEC)*, Sep. 2021, pp. 1–5, doi: 10.1109/AUPEC52110.2021.9597815.

[138] E. Roshandel, A. Mahmoudi, S. Kahourzade, and W. Soong, "Analytical model and performance prediction of induction motors using subdomain technique," in *Proc. ECCE IEEE Energy Convers. Congr. Expo.*, Oct. 2020, pp. 3815–3822, doi: 10.1109/ECCE44975.2020.9235826.

[139] V. T. Tuan, S. Kreuawan, P. Somsiri, and P. N. Huy, "Low cost motor drive technologies for ASEAN electric scooter," *J. Electr. Eng. Technol.*, vol. 13, no. 4, pp. 1578–1585, 2018, doi: 10.5370/JEET.2018.13.4.1578.

[140] M. Novak, J. Novak, and Z. Novak, "Efficiency mapping of a small permanent magnet synchronous motor," in *Proc. Int. Conf. Mechtron.*, in Advances in Intelligent Systems and Computing, vol. 644, 2018, pp. 185–193, doi: 10.1007/978-3-319-65960-2_24.

[141] A. Mahmoudi, W. L. Soong, G. Pellegrino, and E. Armando, "Loss function modeling of efficiency maps of electrical machines," *IEEE Trans. Ind. Appl.*, vol. 53, no. 5, pp. 4221–4231, Sep. 2017, doi: 10.1109/TIA.2017.2695443.

[142] B. A. Nasir, "Modeling of stray losses in equivalent circuit of induction machines," *AIP Conf. Proc.*, vol. 2307, no. 1, Dec. 2020, Art. no. 020006, doi: 10.1063/5.0032902.

[143] P. Pillay, M. Al-Badri, P. Angers, and C. Desai, "A new stray-load loss formula for small and medium-sized induction motors," *IEEE Trans. Energy Convers.*, vol. 31, no. 3, pp. 1221–1227, Sep. 2016, doi: 10.1109/TEC.2016.2539959.

[144] R. Kumar, P. Kumar, T. Kanekawa, and K. Oishi, "Stray loss model for induction motors with using equivalent circuit parameters," *IEEE Trans. Energy Convers.*, vol. 35, no. 2, pp. 1036–1045, Jun. 2020, doi: 10.1109/TEC.2020.2964616.

[145] K. Yamazaki and Y. Haruishi, "Stray load loss analysis of induction motor—Comparison of measurement due to IEEE standard 112 and direct calculation by finite-element method," *IEEE Trans. Ind. Appl.*, vol. 40, no. 2, pp. 543–549, Mar. 2004, doi: 10.1109/tia.2004.824509.

[146] E. Alpaslan, S. A. Çetinkaya, C. Y. Alpaydın, S. A. Korkmaz, M. U. Karaoglan, C. O. Colpan, K. E. Erginer, and A. Gören, "A review on fuel cell electric vehicle powertrain modeling and simulation," *Energy Sources, A, Recovery, Utilization, Environ. Effects*, pp. 1–37, Nov. 2021, doi: 10.1080/15567036.2021.1999347.

[147] M. A. Sakka, J. van Mierlo, H. Gualous, M. A. Sakka, J. van Mierlo, and H. Gualous, "DC/DC converters for electric vehicles," in *Electric Vehicles—Modelling and Simulations*. London, U.K.: IntechOpen, 2011, doi: 10.5772/17048.

[148] C. Wang, H. He, R. Xiong, and Y. Zhang, "A novel efficiency modeling method for a DC–DC converter in the hybrid energy storage system for electric vehicles," *Energy Proc.*, vol. 88, pp. 935–939, Jun. 2016, doi: 10.1016/j.egypro.2016.06.115.

[149] A. Shrivastava and B. Calhoun, "A DC–DC converter efficiency model for system level analysis in ultra low power applications," *J. Low Power Electron. Appl.*, vol. 3, no. 3, pp. 215–232, Jun. 24, 2013, doi: 10.3390/jlpea3030215.

[150] W. Martinez, M. Yamamoto, P. Grbovic, and C. A. Cortes, "Efficiency optimization of a single-phase boost DC–DC converter for electric vehicle applications," in *Proc. 40th Annu. Conf. IEEE Ind. Electron. Soc.*, Oct. 2014, pp. 4279–4285, doi: 10.1109/IECON.2014.7049146.

[151] N. Dias and A. J. Naik, "Design, modeling and simulation of bidirectional buck and boost converter for electric vehicles," in *Proc. Int. Conf. Advancement Technol. (ICONAT)*, Jan. 2022, pp. 1–5, doi: 10.1109/ICONAT53423.2022.9725830.

[152] J. Zhu, H. Kim, H. Chen, R. Erickson, and D. Maksimovic, "High efficiency SiC traction inverter for electric vehicle applications," in *Proc. IEEE Appl. Power Electron. Conf. Exposit. (APEC)*, Mar. 2018, pp. 1428–1433, doi: 10.1109/APEC.2018.8341204.

[153] B. Naourez, N. B. Hadj, R. Abdelmoula, M. Chaieb, and R. Neji. (2018). *Permanent Magnet Motor Efficiency Map Calculation and Small Electric Vehicle Consumption Optimization Electric Vehicles View Project Control Strategies in EV View Project*. [Online]. Available: https://www.researchgate.net/publication/325554576

[154] E. Gurpinar and B. Ozpineci, "Loss analysis and mapping of a SiC MOSFET based segmented two-level three-phase inverter for EV traction systems," in *Proc. IEEE Transp. Electrific. Conf. Expo (ITEC)*, Jun. 2018, pp. 1046–1053, doi: 10.1109/ITEC.2018.8450188.

[155] W. Eberle, Z. Zhang, Y.-F. Liu, and P. C. Sen, "A simple analytical switching loss model for buck voltage regulators," in *Proc. 23rd Annu. IEEE Appl. Power Electron. Conf. Exposit.*, Feb. 2008, pp. 36–42, doi: 10.1109/apec.2008.4522697.

[156] S. Williamson, M. Lukic, and A. Emadi, "Comprehensive drive train efficiency analysis of hybrid electric and fuel cell vehicles based on motor-controller efficiency modeling," *IEEE Trans. Power Electron.*, vol. 21, no. 3, pp. 730–740, May 2006, doi: 10.1109/tpel.2006.872388.

[157] H. Shayeghi, S. Pourjafar, M. Maalandish, and S. Nouri, "Non-isolated DC–DC converter with a high-voltage conversion ratio," *IET Power Electron.*, vol. 13, no. 16, pp. 3797–3806, Dec. 2020, doi: 10.1049/iet-pel.2019.1014.

[158] S. A. Syed, H. A. Khalid, and H. Farooq, "Analysis and efficiency evaluation of non-isolated DC/DC converter with wide input voltage range for PV application," *Eng. Proc.*, vol. 20, no. 1, p. 10, Jul. 2022, doi: 10.3390/ENGPROC2022020010.

[159] R. Zhang, D. Zhang, and R. Dutta, "Study on core loss reduction in the transformer of isolated DC/DC converter with series L-C and resonant L-C shunt filter," in *Proc. Australas. Universities Power Eng. Conf. (AUPEC)*, Nov. 2018, pp. 1–5, doi: 10.1109/AUPEC.2018.8757908.

[160] M.-K. Nguyen, T.-D. Duong, and Y.-C. Lim, "Switched-capacitor-based dual-switch high-boost DC–DC converter," *IEEE Trans. Power Electron.*, vol. 33, no. 5, pp. 4181–4189, May 2018, doi: 10.1109/TPEL.2017.2719040.

[161] S. Salamone, B. Lenzo, G. Lutzemberger, F. Bucchi, and L. Sani, "On the investigation of energy efficient torque distribution strategies through a comprehensive powertrain model," *Sustainability*, vol. 13, no. 8, p. 4549, Apr. 2021, doi: 10.3390/su13084549.

[162] R. Jaschke, "Conduction losses in DC/DC-converters as buckboost/boostbuck synchronous rectifier types," in *Proc. Compat. Power Electron.*, May 2007, pp. 1–5, doi: 10.1109/cpe.2007.4296545.

[163] M. Premkumar, C. Kumar, and R. Sowmya, "Analysis and implementation of high-performance DC–DC step-up converter for multilevel boost structure," *Frontiers Energy Res.*, vol. 7, p. 149, Dec. 2019, doi: 10.3389/FENRG.2019.00149.

[164] I. Jagadeesh and V. Indragandhi, "Review and comparative analysis on DC–DC converters used in electric vehicle applications," *IOP Conf. Ser., Mater. Sci. Eng.*, vol. 623, no. 1, Oct. 2019, Art. no. 012005, doi: 10.1088/1757-899x/623/1/012005.

[165] D. M. Bellur and M. K. Kazimierczuk, "DC–DC converters for electric vehicle applications," in *Proc. Electr. Insul. Conf. Electr. Manuf. Expo*, Oct. 2007, pp. 286–293, doi: 10.1109/eeic.2007.4562633.

[166] T. Huria, M. Ceraolo, J. Gazzarri, and R. Jackey, "High fidelity electrical model with thermal dependence for characterization and simulation of high power lithium battery cells," in *Proc. IEEE Int. Electric Vehicle Conf.*, Mar. 2012, pp. 1–8, doi: 10.1109/IEVC.2012.6183271.

[167] V. V. Shimin, V. A. Shah, and M. M. Lokhande, "Electric vehicle batteries: A selection based on PROMETHEE method," in *Proc. IEEE 7th Power India Int. Conf. (PIICON)*, Nov. 2016, pp. 1–6, doi: 10.1109/POWERI.2016.8077224.

[168] I. Evtimov, R. Ivanov, and M. Sapundjiev, "Energy consumption of auxiliary systems of electric cars," in *Proc. MATEC Web Conferences*, vol. 133, Nov. 2017, pp. 1–9, doi: 10.1051/MATECCONF/201713306002.

[169] M. Vražić, O. Barić, and P. Virtič, "Auxiliary systems consumption in electric vehicle," *Przeglad Elektrotechniczny*, vol. 2014, no. 12, pp. 172–175, Dec. 2014, doi: 10.12915/PE.2014.12.42.

[170] G. Shivhare, K. Kundu, J. Narayan, and S. K. Dwivedy, "Design and modeling of a compact lightweight electric-scooter," in *Proc. Int. Conf. Comput. Perform. Eval. (ComPE)*, Dec. 2021, pp. 944–949, doi: 10.1109/ComPE53109.2021.9752193.

[171] M. Kalolia. (2012). *Modeling, Simulation and Experimental Verification of an Electric Bicycle With Regenerative Braking*. Accessed: Jan. 17, 2023. [Online]. Available: https://engagedscholarship.csuohio.edu/etdarchive/642

[172] S. Singirikonda and Y. P. Obulesu, "Battery modelling and state of charge estimation methods for energy management in electric vehicle—A review," *IOP Conf. Ser., Mater. Sci. Eng.*, vol. 937, no. 1, Sep. 2020, Art. no. 012046, doi: 10.1088/1757-899x/937/1/012046.

[173] *Electric Vehicles and Renewable Energy–Unit 7–Module 5—Fundamentals of Battery Pack Design*. Accessed: Jan. 17, 2023. [Online]. Available: https://onlinecourses.nptel.ac.in/noc21_ee112/unit?unit=58&lesson=172

[174] A. O. Kiyakli and H. Solmaz, "Modeling of an electric vehicle with MATLAB/Simulink," *Int. J. Automot. Sci. Technol.*, vol. 2, no. 4, pp. 9–15, Dec. 2018, doi: 10.30939/ijastech.475477.

[175] S. Patwardhan, R. Bindu, and S. Thale, "Modeling and performance analysis of battery electric vehicle," in *Proc. 2nd Int. Conf. Power Embedded Drive Control (ICPEDC)*, Aug. 2019, pp. 24–29, doi: 10.1109/icpedc47771.2019.9036646.

[176] C. Sunanda, "Modeling and performance analysis of an electric vehicle with MATLAB/simulink," *Int. Res. J. Eng. Technol.*, vol. 7, no. 6, p. 1098, 2008, Accessed: Jan. 17, 2023. [Online]. Available: https://www.irjet.net

[177] P. S. Bhowal and B. Anthonysamy, "Realistic electric motor modelling for electric vehicle performance prediction," SAE, Warrendale, PA, USA, Tech. Papers 2021-26-0152, Sep. 2021, doi: 10.4271/2021-26-0152.

[178] J. Rivera-Barrera, N. Muñoz-Galeano, and H. Sarmiento-Maldonado, "SoC estimation for lithium-ion batteries: Review and future challenges," *Electronics*, vol. 6, no. 4, p. 102, Nov. 2017, doi: 10.3390/electronics6040102.

[179] N. Sockeel, J. Shi, M. Shahverdi, and M. Mazzola, "Sensitivity analysis of the battery model for model predictive control: Implementable to a plug-in hybrid electric vehicle," *World Electric Vehicle J.*, vol. 9, no. 4, p. 45, Nov. 2018, doi: 10.3390/wevj9040045.

[180] Z. S. Shamma, B. Jones, M. Clark, C. Bailey, and M. Harper, "Electric vehicle range prediction estimator (EVPRE)," *Softw. Impacts*, vol. 13, Aug. 2022, Art. no. 100369, doi: 10.1016/j.simpa.2022.100369.

[181] S. A. Hasib, D. K. Saha, S. Islam, M. Tanvir, and M. S. Alam, "Driving range prediction of electric vehicles: A machine learning approach," in *Proc. 5th Int. Conf. Electr. Eng. Inf. Commun. Technol. (ICEEICT)*, Nov. 2021, pp. 1–6, doi: 10.1109/ICEEICT53905.2021.9667927.

[182] A. Amirkhani, A. Haghanifar, and M. R. Mosavi, "Electric vehicles driving range and energy consumption investigation: A comparative study of machine learning techniques," in *Proc. 5th Iranian Conf. Signal Process. Intell. Syst. (ICSPIS)*, Dec. 2019, pp. 1–6, doi: 10.1109/ICSPIS48872.2019.9066042.

[183] M. Waseem, M. Suhaib, and A. F. Sherwani, "Modelling and analysis of gradient effect on the dynamic performance of three-wheeled vehicle system using simscape," *Social Netw. Appl. Sci.*, vol. 1, no. 3, pp. 1–13, Mar. 2019, doi: 10.1007/s42452-019-0235-8.

[184] B. Sharmila, "Modelling and performance analysis of electric vehicle," *Int. J. Ambient Energy*, vol. 43, no. 1, pp. 5034–5040, 2021, doi: 10.1080/01430750.2021.1932587.

[185] M. Gerami Tehrani, J. Kelkka, J. Sopanen, A. Mikkola, and K. Kerkkänen, "Electric vehicle energy consumption simulation by modeling the efficiency of driveline components," *SAE Int. J. Commercial Vehicles*, vol. 9, no. 1, pp. 31–39, Apr. 2016, doi: 10.4271/2016-01-9016.

[186] M. Khan Tal, V. Balyan, and B. Groenewald, "A simulation study of power and energy requirements of an electric vehicle for hybridisation purposes," *SSRN Electron. J.*, Nov. 2019, doi: 10.2139/ssrn.3657035.

[187] N. V. Martyushev, B. V. Malozyomov, S. N. Sorokova, E. A. Efremenkov, and M. Qi, "Mathematical modeling the performance of an electric vehicle considering various driving cycles," *Mathematics*, vol. 11, no. 11, p. 2586, Jun. 2023, doi: 10.3390/math11112586.

[188] A. Bhatt, "Planning and application of electric vehicle with MATLAB®/Simulink®," in *Proc. IEEE Int. Conf. Power Electron., Drives Energy Syst. (PEDES)*, Dec. 2016, pp. 1–6, doi: 10.1109/PEDES.2016.7914220.

[189] T. P. Mish-Al, P. G. A. Mani, and A. K. Parvathy, "Development of electric vehicle model in MATLAB/simulink," in *Proc. 8th Int. Conf. Smart Struct. Syst. (ICSSS)*, Apr. 2022, pp. 01–07, doi: 10.1109/ICSSS54381.2022.9782171.

[190] N. Lokhande, A. Deore, J. Dinani, and N. Sayed, "Range estimation of electric vehicle using MATLAB," in *Proc. 6th Int. Conf. for Converg. Technol. (I2CT)*, Apr. 2021, pp. 1–6, doi: 10.1109/I2CT51068.2021.9417876.

[191] M. A. Halabi and A. A. Tarabsheh, "Modelling of electric vehicles using MATLAB/Simulink," SAE Int., Warrendale, PA, USA, SAE Tech. Papers 2020-01-5086, 2020, doi: 10.4271/2020-01-5086.

[192] K. Vijayakumar, R. Bhuvhanesan, M. Devadharshini, C. O. S. Reddy, and S. Kannan, "Analysis of performance parameters of electric vehicle using MATLAB simulink," in *Proc. 2nd Int. Conf. Advance Comput. Innov. Technol. Eng. (ICACITE)*, Apr. 2022, pp. 1465–1471, doi: 10.1109/ICACITE53722.2022.9823742.

[193] K. Mahmud and G. E. Town, "A review of computer tools for modeling electric vehicle energy requirements and their impact on power distribution networks," *Appl. Energy*, vol. 172, pp. 337–359, Jun. 2016, doi: 10.1016/j.apenergy.2016.03.100.

[194] W. J. Sweeting, A. R. Hutchinson, and S. D. Savage, "Factors affecting electric vehicle energy consumption," *Int. J. Sustain. Eng.*, vol. 4, no. 3, pp. 192–201, Sep. 2011, doi: 10.1080/19397038.2011.592956.

[195] A. Skuza and R. S. Jurecki, "Analysis of factors affecting the energy consumption of an EV vehicle—A literature study," *IOP Conf. Ser., Mater. Sci. Eng.*, vol. 1247, no. 1, Jul. 2022, Art. no. 012001, doi: 10.1088/1757-899x/1247/1/012001.

[196] S. Anu and R. Manjunatha, "Design and modelling of ultra-capacitor based hybrid energy storage system in electric two-wheeler for Indian driving cycle," in *Proc. IEEE Int. Conf. Distrib. Comput. Electr. Circuits Electron. (ICDCECE)*, India, Apr. 2022, pp. 1–7, doi: 10.1109/ICDCECE53908.2022.9793082.

[197] H. A. Chari and D. R. Katikar, "Mathematical modeling of the electric scooter battery pack using SCILAB," *Int. J. Advance Res., Ideas Innov. Technol.*, vol. 8, no. 1, pp. 252–257, 2022.

[198] S. Wankhede, P. Thorat, S. Shisode, S. Sonawane, and R. Wankhade, "Energy consumption estimation for electric two-wheeler using different drive cycles for achieving optimum efficiency," *Energy Storage*, vol. 4, no. 6, Dec. 2022, doi: 10.1002/est2.361.

[199] M. N. Yuniarto, I. Sidharta, S. E. Wiratno, Y. U. Nugraha, and D. A. Asfani, "Indonesian electric motorcycle development: Lessons from innovation-based concept implementation on the design and production of the first Indonesian electric motorcycle," *IEEE Electrific. Mag.*, vol. 10, no. 1, pp. 65–74, Mar. 2022, doi: 10.1109/MELE.2021.3139247.

[200] H. F. Gharibeh and A. S. Yazdankhah, "Efficiency improvement of a directly-driven electric scooter with energy management and battery sizing," in *Proc. 3rd Conf. Renew. Energies Distrib. Gener.*, 2013, pp. 1–9, Accessed: Jan. 18, 2023. [Online]. Available: https://fardapaper.ir/mohavaha/uploads/2017/09/4_448416146438231793.pdf

[201] R. Sreejith and K. R. Rajagopal, "An insight into motor and battery selections for three-wheeler electric vehicle," in *Proc. IEEE 1st Int. Conf. Power Electron., Intell. Control Energy Syst. (ICPEICES)*, Jul. 2016, pp. 1–6, doi: 10.1109/ICPEICES.2016.7853494.

[202] O. Tade and J. Kale, "Sizing and simulation of powertrain of three-wheeler electric vehicle," *Int. J. Eng. Sci.*, vol. 14, no. 3, 2021, doi: 10.36224/ijes.140304.

[203] S. D. Vidhya and M. Balaji, "Modelling, design and control of a light electric vehicle with hybrid energy storage system for Indian driving cycle," *Meas. Control*, vol. 52, nos. 9–10, pp. 1420–1433, Nov. 2019, doi: 10.1177/0020294019858212.

[204] P. Mishra, S. Saha, and H. P. Ikkurti, "A methodology for selection of optimum power rating of propulsion motor of three wheeled electric vehicle on Indian drive cycle (IDC)," *Int. J. Theor. Appl. Res. Mech. Eng.*, vol. 2, no. 1, pp. 1–16, 2013.

[205] I. Miri, A. Fotouhi, and N. Ewin, "Electric vehicle energy consumption modelling and estimation—A case study," *Int. J. Energy Res.*, vol. 45, no. 1, pp. 501–520, Jan. 2021, doi: 10.1002/er.5700.

[206] C. Xu, J. Niu, and F. Pei, "Design and simulation of the power-train system for an electric vehicle," in *Proc. 2nd Int. Conf. Artif. Intell., Manag. Sci. Electron. Commerce (AIMSEC)*, 2011, pp. 3868–3871, doi: 10.1109/AIMSEC.2011.6010059.

[207] P. D. Walker, S. A. Rahman, B. Zhu, and N. Zhang, "Modelling, simulations, and optimisation of electric vehicles for analysis of transmission ratio selection," *Adv. Mech. Eng.*, vol. 2013, Jan. 2013, Art. no. 340435, doi: 10.1155/2013/340435.

[208] M. Zhou, L. Zhao, Y. Zhang, Z. Gao, and R. Pei, "Pure electric vehicle power-train parameters matching based on vehicle performance," *Int. J. Control Autom.*, vol. 8, no. 9, pp. 53–62, Sep. 2015, doi: 10.14257/ijca.2015.8.9.06.

[209] G. Wu, X. Zhang, and Z. Dong, "Impacts of two-speed gearbox on electric vehicle's fuel economy and performance," SAE, Warrendale, PA, USA, Tech. Papers 2013-01-0349, vol. 2, Apr. 2013, doi: 10.4271/2013-01-0349.

[210] I. Pielecha and J. Pielecha, "Simulation analysis of electric vehicles energy consumption in driving tests," *Eksploatacja i Niezawodność Maintenance Rel.*, vol. 22, no. 1, pp. 130–137, Mar. 2020, doi: 10.17531/ein.2020.1.15.

[211] G. Wager, J. Whale, and T. Braunl, "Driving electric vehicles at highway speeds: The effect of higher driving speeds on energy consumption and driving range for electric vehicles in Australia," *Renew. Sustain. Energy Rev.*, vol. 63, pp. 158–165, Sep. 2016, doi: 10.1016/j.rser.2016.05.060.

[212] S. Kremzow-Tennie, M. Hellwig, and F. Pautzke, "A study on the influencing factors regarding energy consumption of electric vehicles," in *Proc. 21st Int. Conf. Res. Educ. Mechatronics (REM)*, Dec. 2020, pp. 1–6, doi: 10.1109/REM49740.2020.9313934.

[213] W. Danek, "Determination of the drag coefficient high performance electric vehicle," *Modelowanie Inżynierskie*, vol. 52, pp. 1–6, Jan. 2014.

[214] F. Badin, F. Le Berr, H. Briki, J-C. Dabadie, M. Petit, S. Magand, and E. Condemine, "Evaluation of EVs energy consumption influencing factors, driving conditions, auxiliaries use, driver's aggressiveness," in *Proc. World Electr. Vehicle Symp. Exhib. (EVS27)*, Nov. 2013, pp. 1–12, doi: 10.1109/EVS.2013.6914723.

[215] A. T. De Almeida, F. J. T. E. Ferreira, and J. A. C. Fong, "Standards for efficiency of electric motors," *IEEE Ind. Appl. Mag.*, vol. 17, no. 1, pp. 12–19, Jan. 2011, doi: 10.1109/mias.2010.939427.

[216] J. Ruan, P. Walker, and N. Zhang, "A comparative study energy consumption and costs of battery electric vehicle transmissions," *Appl. Energy*, vol. 165, pp. 119–134, Mar. 2016, doi: 10.1016/j.apenergy.2015.12.081.

[217] K. Kambly and T. H. Bradley, "Geographical and temporal differences in electric vehicle range due to cabin conditioning energy consumption," *J. Power Sources*, vol. 275, pp. 468–475, Feb. 2015, doi: 10.1016/j.jpowsour.2014.10.142.

[218] T. Yuksel and J. J. Michalek, "Effects of regional temperature on electric vehicle efficiency, range, and emissions in the United States," *Environ. Sci. Technol.*, vol. 49, no. 6, pp. 3974–3980, Mar. 2015, doi: 10.1021/ES505621S.

[219] E. Yao, Z. Yang, Y. Song, and T. Zuo, "Comparison of electric vehicle's energy consumption factors for different road types," *Discrete Dyn. Nature Soc.*, vol. 2013, pp. 1–7, 2013, doi: 10.1155/2013/328757.

[220] Y. Ramanujam, I. Malhotra, and S. Thimmalapura, "A study of parameters influencing energy consumption of an electric vehicle," in *Proc. IEEE Transp. Electrific. Conf. (ITEC-India)*, India, Dec. 2019, pp. 1–6, doi: 10.1109/ITEC-India48457.2019.ITECINDIA2019-45.

[221] J. Hofer, E. Wilhelm, and W. Schenler, "Comparing the mass, energy, and cost effects of lightweighting in conventional and electric passenger vehicles," *J. Sustain. Develop. Energy, Water Environ. Syst.*, vol. 2, no. 3, pp. 284–295, Sep. 2014.

[222] D. Berjoza and I. Jurgena, "Influence of batteries weight on electric automobile performance," *Eng. Rural Develop.*, vol. 16, pp. 1388–1394, Mar. 2017, doi: 10.22616/ERDEV2017.16.N316.

[223] R. Zhi-yong, "Research on influence factors affecting driving range of flame-proof battery electric vehicles," in *Proc. IEEE 4th Adv. Inf. Technol., Electron. Autom. Control Conf. (IAEAC)*, vol. 1, Dec. 2019, pp. 1982–1986, doi: 10.1109/IAEAC47372.2019.8997686.

[224] A. Donkers, D. Yang, and M. Viktorovic, "Influence of driving style, infrastructure, weather and traffic on electric vehicle performance," *Transp. Res. D, Transp. Environ.*, vol. 88, Nov. 2020, Art. no. 102569, doi: 10.1016/j.trd.2020.102569.

[225] K. Liu, J. Wang, T. Yamamoto, and T. Morikawa, "Modelling the multilevel structure and mixed effects of the factors influencing the energy consumption of electric vehicles," *Appl. Energy*, vol. 183, pp. 1351–1360, Dec. 2016, doi: 10.1016/j.apenergy.2016.09.082.
[226] Y. Wu, Z. Huang, Y. Zheng, Y. Liu, H. Li, Y. Che, J. Peng, and R. Teodorescu, "Spatial–temporal data-driven full driving cycle prediction for optimal energy management of battery/supercapacitor electric vehicles," *Energy Convers. Manage.*, vol. 277, Feb. 2023, Art. no. 116619, doi: 10.1016/j.enconman.2022.116619.
[227] K. Unni and S. Thale, "Simulation and analysis of factors influencing the residual range of electric vehicle," in *Proc. IEEE Bombay Sect. Signature Conf. (IBSSC)*, Nov. 2021, pp. 1–6, doi: 10.1109/IBSSC53889.2021.9673171.
[228] Z. Yi and P. H. Bauer, "Effects of environmental factors on electric vehicle energy consumption: A sensitivity analysis," *IET Electr. Syst. Transp.*, vol. 7, no. 1, pp. 3–13, Mar. 2017, doi: 10.1049/iet-est.2016.0011.
[229] K. Sarrafan, D. Sutanto, K. M. Muttaqi, and G. Town, "Accurate range estimation for an electric vehicle including changing environmental conditions and traction system efficiency," *IET Electr. Syst. Transp.*, vol. 7, no. 2, pp. 117–124, Jun. 2017, doi: 10.1049/iet-est.2015.0052.
[230] W. Gołębiewski, "Theoretical analysis of the effect of traction parameters on electric vehicle energy consumption and driving range," *Gołębiewski, Wawrzyniec*, vol. 16, no. 1, pp. 343–354, 2016, doi: 10.2/JQUERY.MIN.JS.
[231] P. Spanoudakis, G. Moschopoulos, T. Stefanoulis, N. Sarantinoudis, E. Papadokokolakis, I. Ioannou, S. Piperidis, L. Doitsidis, and N. C. Tsourveloudis, "Efficient gear ratio selection of a single-speed drivetrain for improved electric vehicle energy consumption," *Sustainability*, vol. 12, no. 21, p. 9254, Nov. 2020, doi: 10.3390/su12219254.
[232] D. Chandran and M. Joshi, "Electric vehicles and driving range extension—A literature review," *Adv. Automobile Eng.*, vol. 5, no. 2, pp. 1–10, 2016, doi: 10.4172/2167-7670.1000154.
[233] S. Vignesh, Y. K. Bhateshvar, M. R. B. Agrewale, and K. C. Vora, "Comparative analysis of powertrain optimization for small electric vehicle based on range and weight for retro-fitment," *Mater. Today: Proc.*, vol. 63, pp. 579–586, Jan. 2022, doi: 10.1016/j.matpr.2022.04.043.
[234] G. Xiao, Q. Chen, P. Xiao, L. Zhang, and Q. Rong, "Multiobjective optimization for a Li-ion battery and supercapacitor hybrid energy storage electric vehicle," *Energies*, vol. 15, no. 8, p. 2821, Apr. 2022, doi: 10.3390/en15082821.
[235] M. R. Çorapsiz and H. Kahveci, "Double adaptive power allocation strategy in electric vehicles with battery/supercapacitor hybrid energy storage system," *Int. J. Energy Res.*, vol. 46, no. 13, pp. 18819–18838, Oct. 2022, doi: 10.1002/er.8501.
[236] M. B. F. Ahsan, S. Mekhilef, T. K. Soon, M. B. Mubin, P. Shrivastava, and M. Seyedmahmoudian, "Lithium-ion battery and supercapacitor-based hybrid energy storage system for electric vehicle applications: A review," *Int. J. Energy Res.*, vol. 46, no. 14, pp. 19826–19854, Nov. 2022, doi: 10.1002/er.8439.
[237] A. K. M. Ahasan Habib, M. Kamrul Hasan, S. Islam, R. Sharma, R. Hassan, N. Nafi, K. Yadav, and S. Dlaim Alotaibi, "Energy-efficient system and charge balancing topology for electric vehicle application," *Sustain. Energy Technol. Assessments*, vol. 53, Oct. 2022, Art. no. 102516, doi: 10.1016/j.seta.2022.102516.
[238] W. Cai, X. Wu, M. Zhou, Y. Liang, and Y. Wang, "Review and development of electric motor systems and electric powertrains for new energy vehicles," *Automot. Innov.*, vol. 4, no. 1, pp. 3–22, Feb. 2021, doi: 10.1007/S42154-021-00139-Z.
[239] Y. Wang and D. Sun, "Powertrain matching and optimization of dual-motor hybrid driving system for electric vehicle based on quantum genetic intelligent algorithm," *Discrete Dyn. Nature Soc.*, vol. 2014, pp. 1–11, 2014, doi: 10.1155/2014/956521.
[240] M. S. H. Lipu, M. S. Miah, S. Ansari, S. T. Meraj, K. Hasan, R. M. Elavarasan, A. A. Mamun, M. A. A. M. Zainuri, and A. Hussain, "Power electronics converter technology integrated energy storage management in electric vehicles: Emerging trends, analytical assessment and future research opportunities," *Electronics*, vol. 11, no. 4, p. 562, Feb. 2022, doi: 10.3390/electronics11040562.
[241] H. Won, Y.-K. Hong, M. Choi, J. Platt, B. Bryant, S. Choi, S. Li, H.-S. Yoon, T. A. Haskew, J. Lee, T. Lee, and T.-W. Lim, "Novel design of six-phase spoke-type ferrite permanent magnet motor for electric truck application," *Energies*, vol. 15, no. 6, p. 1997, Mar. 2022, doi: 10.3390/en15061997.
[242] S. Singh, K. P. Tiwari, A. Shahi, M. N. Singh, and S. Tripathi, "Efficiency improvement for regenerative braking system for a vehicular model using supercapacitor," in *Machine Learning, Advances in Computing, Renewable Energy and Communication* (Lecture Notes in Electrical Engineering), vol. 768. Singapore: Springer, 2022, pp. 327–340, doi: 10.1007/978-981-16-2354-7_30.
[243] P. Stabile, F. Ballo, G. Mastinu, and M. Gobbi, "An ultra-efficient lightweight electric vehicle—Power demand analysis to enable lightweight construction," *Energies*, vol. 14, no. 3, p. 766, Feb. 2021, doi: 10.3390/en14030766.
[244] Z. Pusztai, P. Kőrös, and F. Friedler, "Vehicle model for driving strategy optimization of energy efficient lightweight vehicle," *Chem. Eng. Trans.*, vol. 88, pp. 385–390, Nov. 2021, doi: 10.3303/CET2188064.
[245] J. T. J. Burd, E. A. Moore, H. Ezzat, R. Kirchain, and R. Roth, "Improvements in electric vehicle battery technology influence vehicle lightweighting and material substitution decisions," *Appl. Energy*, vol. 283, Feb. 2021, Art. no. 116269, doi: 10.1016/j.apenergy.2020.116269.
[246] J. Ma, Y. Sun, S. Zhang, J. Li, and S. Li, "Experimental study on the performance of vehicle integrated thermal management system for pure electric vehicles," *Energy Convers. Manage.*, vol. 253, Feb. 2022, Art. no. 115183, doi: 10.1016/j.enconman.2021.115183.
[247] V. Bijina, P. J. Jandas, S. Joseph, J. Gopu, K. Abhitha, and H. John, "Recent trends in industrial and academic developments of green tyre technology," *Polym. Bull.*, vol. 80, no. 8, pp. 8215–8244, Sep. 2022, doi: 10.1007/s00289-022-04445-2.
[248] C. Fiori, V. Marzano, V. Punzo, and M. Montanino, "Energy consumption modeling in presence of uncertainty," *IEEE Trans. Intell. Transp. Syst.*, vol. 22, no. 10, pp. 6330–6341, Oct. 2021, doi: 10.1109/TITS.2020.2991270.
[249] J. Asamer, A. Graser, B. Heilmann, and M. Ruthmair, "Sensitivity analysis for energy demand estimation of electric vehicles," *Transp. Res. D, Transp. Environ.*, vol. 46, pp. 182–199, Jul. 2016, doi: 10.1016/j.trd.2016.03.017.

AZHAGANATHAN GURUSAMY received the M.E. degree in internal combustion engineering from Anna University, Chennai. He is currently pursuing the Ph.D. degree with the Vellore Institute of Technology (VIT), Vellore, Tamil Nadu. His research focuses mainly on the development of electric vehicle testing standards, advanced EV powertrains, and real-time testing of EV. His research interests include conventional, hybrid, and pure electric vehicle analysis in local driving conditions.

BRAGADESHWARAN ASHOK received the Ph.D. degree from the School of Mechanical Engineering, Vellore Institute of Technology (VIT), Vellore. He is currently an Associate Professor with the Department of Automotive Technology, School of Mechanical engineering, VIT. His research work is aimed towards the motor control algorithm development for electric vehicle application. His research interests include automotive engineering, electric and hybrid vehicle powertrain calibration, IC engines, and automotive electronics. He has been awarded as "Top 2% Scientist in the World" by a study conducted from researchers of Stanford University recently.

BYRON MASON received the B.Eng. degree in mechanical engineering and the Ph.D. degree in powertrain calibration and control from the University of Bradford, Bradford, U.K., in 2005 and 2009, respectively. He is currently a Senior Lecturer in intelligent powertrain systems with the Department of Aeronautical and Automotive Engineering, Loughborough University, Loughborough, U.K.